EXPERIMENTAL STUDY ON DROPLET FORMATION USING A NEWTONIAN AND A NON-NEWTONIAN LIQUID FLOWING IN A MICROCHANNEL SUBJECT TO AN AC ELECTRIC FIELD

by

Yiğit Ağanoğlu

B.S., Chemical Engineering, Boğaziçi University, 2016

Submitted to the Institute for Graduate Studies in
Science and Engineering in partial fulfillment of
the requirements for the degree of
Master of Science

Graduate Program in Chemical Engineering

Boğaziçi University

2019

ACKNOWLEDGEMENTS

First, I would like to express my deep gratitude to Assoc. Prof. A. Kerem Uğuz, my thesis supervisor, for his patient guidance, enthusiastic encouragement, useful critiques and offering his extensive knowledge and expertise on the subject.

I wish to express my sincere appreciation to the members of the thesis committee, Prof. A. Erhan Aksoylu and Assoc. Prof. Erdem Günay, for accepting to be members, devoting their valuable time to read and comment on my thesis.

I would like to thank Sercan Altundemir for his instruction and assistance from the beginning of this work. Also, very special thanks to my lab partners Pınar Eribol and Seymen İlke Kaykanat for their help and guidance whenever I needed them.

I would like to extend my thanks to Gamze Kabadayı, Başak Aygören and Meryem İriş for their unwavering optimism, trust in my endeavors and friendship through my M.Sc. years.

I would also like to extend my thanks to Bensu Poslu and Selma Başıbüyük for their hospitality and support essential to the fruition of this work when I needed them the most.

Cordial thanks to Dilek Kırkoç, Şükrü Ordu, Yakup Bal and Murat Düzgünoğlu for their technical assistance and help.

Finally, I wish to thank my parents for their wise counsel, sympathetic ear and unquestioning faith in my endeavors.

Boğaziçi University Research Fund Grant Number 14000 and TÜBİTAK Project 116M374 are acknowledged for the financial support.

ABSTRACT

EXPERIMENTAL STUDY ON DROPLET FORMATION USING A NEWTONIAN AND A NON-NEWTONIAN LIQUID FLOWING IN A MICROCHANNEL SUBJECT TO AN AC ELECTRIC FIELD

The aim of this work is to experimentally investigate the electrohydrodynamic instability and droplet formation between two immiscible liquids flowing in a microchannel. When two immiscible liquids are pumped into a microchannel, a flat stable interface forms between them because of the laminar regime of the flow. If an external electric field is applied in a direction normal to the interface, the interface may deflect and deform. This phenomenon is called the electrohydrodynamic (EHD) instability and can be used for the generation and the manipulation of droplets. The volumes of droplets generated in this work are in the range of 0.4 to 1.5 μL. For the experiments in this study, handmade microchannels that are 1.10 mm in width and 0.36 or 0.55 mm in depth with an electrode length of 10 or 20 mm are used. For the investigation of the EHD instability between two Newtonian liquids, silicone oil with a kinematic viscosity of 50 cSt is used as the dispersed phase and ethylene glycol (EG) is used as the continuous phase; where the applied electric field is normal to the interface and in the range of 0.68 to 2.18 kV. For the EHD instability analysis for the interface between a Newtonian and a non-Newtonian liquid, the dispersed phase is kept the same and the continuous phase is replaced with a xanthan gum/aqueous glycerol solution; and the applied voltages are in the range of 0.54 to 2.73 kV. Finally, the formation of silicone oil droplets in the non-Newtonian phase and the droplet size dependency on the thickness ratio and the applied voltage are studied. The applied voltages for the generation of droplets are above the critical voltage of the system and range from 0.96 to 3.53 kV.

ÖZET

BİR MİKROKANALDA AKAN VE ALTERNATİF ELEKTRİK ALANA TABİ TUTULAN BİR NEWTONYEN VE BİR NEWTONYEN OLMAYAN SIVIDAN DAMLACIK OLUŞUMU ÜZERİNE DENEYSEL ÇALIŞMA

Bu çalışmanın amacı, bir mikrokanal içinde akan iki karışmayan sıvı arasındaki elektrohidrodinamik kararsızlığı ve damlacık oluşumunu deneysel olarak incelemektir. İki karışmayan sıvı bir mikrokanalın içine pompalandığında, akışın laminer rejiminden dolayı aralarında düz ve kararlı bir arayüzey meydana gelir. Harici bir elektrik alan, arayüzeye dik bir yönde uygulanırsa, arayüzey bozulabilir ve deforme olabilir. Bu fenomene elektrohidrodinamik (EHD) kararsızlık denir ve damlacıkların oluşumu ve manipülasyonu için kullanılabilir. Bu çalışmada üretilen damlacıkların hacmi 0.4 ila 1.5 μL aralığındadır. Bu çalışmada yapılan deneylerde, 10 veya 20 mm elektrot uzunluğunda 1.10 mm genişliğinde ve 0.36 veya 0.55 mm derinliğinde el yapımı mikrokanallar kullanılmıştır. İki Newtonyen sıvı arasındaki EHD kararsızlığın araştırılması için, dağılmış faz olarak 50 cSt kinematik viskoziteli silikon yağı ve sürekli faz olarak etilen glikol (EG) kullanılmıştır; uygulanan elektrik alan arayüzeye normaldir ve büyüklüğü 0.68 ila 2.18 kV aralığındadır. Newtonian bir sıvı ile Newtonian olmayan bir sıvı arasındaki arayüzeyin EHD kararsızlık analizi için, dağınık faz aynı tutulup sürekli faz bir ksantan sakızı / sulu gliserol çözeltisi ile değiştirilip; uygulanan gerilimler, 0.54 ila 2.73 kV aralığında kalmıştır. Son olarak, Newtonyen olmayan fazda silikon yağı damlacıklarının oluşumu ve damlacık büyüklüğünün kalınlık oranına ve uygulanan gerilime bağlılığı incelenmiştir. Damlacıkların oluşması için uygulanan gerilimler sistemin kritik geriliminin üstündedir ve 0.96 ila 3.53 kV arasındadır.

TABLE OF CONTENTS

LIST OF FIGURES

LIST OF TABLES

LIST OF SYMBOLS

d_d	Droplet diameter
D_f	Frequency of droplet formation
f	Frequency of the applied electric field
H_1	Thickness of the dispersed phase
H_2	Thickness of the continuous phase
H_r	Thickness ratio
L_i	Interfacial contact length
Q_1	Volumetric flow rate of the dispersed phase
Q_2	Volumetric flow rate of the continuous phase
Q_r	Volumetric flow rate ratio
Q_T	Total volumetric flow rate
V	Applied voltage
V_c	Critical voltage
$V_{droplet}$	Droplet volume
ε_r	Permittivity ratio
μ_r	Viscosity ratio
σ_r	Conductivity ratio

LIST OF ACRONYMS/ABBREVIATIONS

AC	Alternating current
DC	Direct current
EG	Ethylene glycol
EHD	Electrohydrodynamic
N-N	Newtonian / Newtonian system
N-nN	Newtonian / non-Newtonian system
PCR	Polymerase chain reaction
PMMA	Poly(methyl methacrylate)
XG/AGl	250 ppm xanthan gum / 85% aqueous glycerol solution

1. INTRODUCTION

Microfluidics is the study of systems that involve processing and/or manipulation of small (10^{-18} to 10^{-9} liters) amounts of fluids using channels whose dimensions are on the order of magnitude of tens to hundreds of micrometers[1]. These systems provide several useful capabilities such as the ability to analyze small amounts of samples and reagents, high resolution and sensitive separations[2] and detections[3], measurements of physical properties such as viscosity[4], pH[5] and fluid density[6], control over chemical[7] or biological[8] reactions, lowered costs, shortened periods of time for analyses and small footprint measurement devices[1]. Their applications in science can extend as far as cell culturing[9], polymerase chain reaction[10] and immunoassay[11].

One branch of microfluidics is the study of multiphase flows in microchannels that enables generation and manipulation of monodisperse droplets in a continuous liquid stream[1][12]. It should be considered that flows in microchannels are, in most cases, laminar with very low Reynolds number[13]. In addition, the fluid transport inside a microchannel is mostly due to the bulk motion of the fluid, pointing to high Péclet number. This means, the liquids do not display turbulent behavior and it becomes problematic to mix them in a desired fashion since the conventional methods for large scales fail to do so[14]. To solve the problem of mixing, several novel methods were proposed throughout years such as passive droplet formation via breakup in co-flowing streams, T-Junction[15] and flow-focusing[16]; and active droplet generation via application of an external electric field[17]. The motion of these droplets inside microchannels can be pressure-driven, thermally driven or electrically driven. It has been shown that these droplets with controlled sizes, size distributions and frequencies[18] can function as actuators for pumping a primary flow or driving mixing flows, individual “chemical reactors” and emulsions[19]. Generation of droplets inside a microchannel in a controlled manner has many applications such as those in production of polymer particles, emulsions and foams, cell biology, chemical synthesis (especially in organic and medicinal chemistry) and microanalysis[1].

In practice, these monodisperse droplets have been utilized in various applications such as polymerase chain reaction (PCR) amplification, synthetic biology and exploration

of cellular-membrane processes. In PCR amplification, droplets serve as discrete compartments that can accommodate certain reactions taking place in parallel and their associated reagents, thereby increasing the efficiency of amplification and eliminating reagent dispersion into the stream and reagent adsorption on microchannel surfaces. In addition, droplets are used to emulate the functioning of lipid bilayers which regulate the activities of membrane bound compounds such as transmembrane proteins and ion channels. This application is held in the study of cellular-membrane processes since droplet interface bilayers can successfully mimic the properties of lipid bilayers in a controlled fashion and environment[20].

Droplet formation inside a microchannel can be induced via active methods. One of the active methods is the introduction of an external electric field to the system. In the presence of an external electric field, the flat interface between two immiscible liquids remains stable up to a certain voltage—called the “critical voltage”. At this point, the interface between the liquids starts to distort and deflect, forming periodic wave patterns. At or above the critical voltage, one of the said liquids forms droplets (the dispersed phase) that are encapsulated within the other liquid (the continuous phase)[21].

In this study, the interfacial instability between two liquid streams flowing in a microchannel is experimentally investigated. The experiments were conducted in two stages. In the first stage, the change in the position of the interface between two Newtonian liquids is measured with respect to the change in their volumetric flow rates. After the flow inside the microchannel is fully developed, that is, when a flat interface at a fixed position is obtained, an external AC electric field is applied to the streams and the critical voltage for a certain configuration of the system is measured.

In the following step, the continuous phase is replaced with a non-Newtonian liquid and once again the position of the interface between two liquid streams is measured at different inlet volumetric flow rates of the incoming phases. The critical voltage of each configuration is measured. The applied voltage is increased beyond the critical voltage of a given configuration to observe formation of droplets of the dispersed phase. The average droplet size for each configuration is measured. The droplet size behavior at varying values of the applied electric field is observed.

2. LITERATURE SURVEY

In this section, the electrohydrodynamic instability phenomenon and the leaky dielectric model are reviewed. The previous work on the topic and different implementations are assessed and presented. The effect of distinct approaches on the matter such as the direction of the applied electric field, the utilization of either a DC or an AC electric field and the choice of liquids are explained in detail. The electrohydrodynamic instability between two liquids and the resulting droplet formation from a Newtonian and a non-Newtonian liquid are investigated in our work.

2.1. Electrohydrodynamic Instability

Electrohydrodynamics is the study of fluid motion induced by electric fields. The behavior/deformation of droplets when exposed to a steady electric field was explained in the mid-1960s by G.I. Taylor via the leaky dielectric model, which is then used by J.R. Melcher to be developed further into electrohydrodynamics (EHD). Although the early experimental studies agreed with the model mostly on a qualitative level, the more recent ones show that this model is in better agreement with real-life applications. Namely, the model can be employed to investigate suspensions as opposed to the prior vision that it can only be applied to sharp interfaces[22].

Linear stability of a two-fluid system has been studied by Abdella and Rasmussen[23], where both phases are unbound and have distinct physical properties such as viscosity, density and conductivity at the interface. The interface between two liquids is subjected to an initially perpendicular electric field. The numerical analysis presents a parameter dependent stability of the said interface. Some of the controlled parameters in the study are viscosity ratio, permittivity ratio, conductivity ratio, density ratio and velocity of the upper fluid in the unperturbed motion.

In one study, Ozen *et al.*[24] showed that droplets can be formed inside a microchannel between two immiscible liquids, and the droplet size can be affected by certain parameters such as the base flow rate and the applied voltage. In this work, corn oil is used as the

continuous phase and glycerin as the dispersed phase. Both liquids are pumped into a T-shaped microchannel where an electric field is applied normal to the flat interface between the said liquids. It has been observed that, when the applied voltage is sufficiently high, flapping of the dispersed phase against the wall of the microchannel and a consequent slug and droplet formation occur. Two sets of data (for two different base flow rates) have been collected from the experiments and the results of both evince a negative correlation between the voltage applied and the size of the droplets formed, i.e. as the applied voltage increases, size of the droplets decreases. It has also been shown that, when the volumetric flow rate of glycerin increases, size of the droplets formed decreases. In addition, it has been reported that the external electric field can induce periodic formation of droplets and their sizes can be controlled within about 1%, e.g. when the applied voltage in this setup is 271.5 V, the mean droplet size is 0.5715 µL with a standard deviation of 0.0016 µL.

In Altundemir *et al.*[21], the interfacial instability between two immiscible Newtonian liquids is experimentally investigated. It is observed that the liquids form a flat interface in a PMMA microchannel and when subjected to a DC electric field, a deflection of the flat interface occurs. In the experiments, ethylene glycol and silicone oil of different kinematic viscosities are chosen as the liquids. The critical voltage (V_c) at which the destabilization of the interface occurs is measured and the effect of certain parameters, such as the thickness ratio (H_r) and the viscosity ratio (μ_r), on the critical voltage is further investigated and empirically formulized. The results show that there is a positive and non-linear correlation between V_c and μ_r for a given depth ratio, which is also in agreement with the work of Li *et al.* The critical voltage gradually increases for low viscosity ratios and plateaus out at higher ones. Critical voltage seems to exhibit a similar pattern against the depth ratio. V_c increases at low thickness ratios and eventually flattens out. Both these results are linked to the stabilizing effect of silicone oils of higher kinematic viscosities. One more conclusion of the study is that the total flow rate (Q_T) has virtually no effect on the critical voltage. For given viscosity and thickness ratios, critical voltage remained the same no matter how high the total flow rate was raised. The final observation in the experiments was slug formation and slug size behavior against μ_r, H_r, and Q_T. It was shown that a periodic slug formation between two Newtonian liquids in a microchannel is possible when the flow is subjected to a DC electric field and the applied voltage is above the critical voltage of the system. The empirical equation, that calculates slug size as a function of H_r, μ_r and Q_T, proposed in the paper shows

that all mentioned parameters have a negative effect on the droplet size, which means an increase in any of the parameters causes a decrease in the droplet size.

2.2. The Leaky Dielectric Model

Studies has shown that exposing a thin liquid film to a DC electric fields can cause the interface to become unstable and form a series of pillars. A further investigation into this phenomenon is one that involves the usage of an AC electric field which has the possibility of exerting better control on both the size and the shape of these pillars. When the film is assumed to be leaky dielectric, linear and non-linear stability analyses show that a high frequency electric field can result in a better manipulation of the patterns formed[25].

In Uguz *et al.*[26], the effect of an electric field—either parallel or normal to the flat interface between two immiscible leaky dielectric liquids flowing in a microchannel—is theoretically analyzed. The analysis suggests that the surface tension has always a stabilizing effect. The effect of the electric field, however, varies based on the nature of its collaboration with the surface tension. Owing to this observation, the conductivity ratio (σ_r) vs. permittivity ratio (ε_r) graph is plotted and the regions where the electric field has a destabilizing effect are labeled. This conclusion was obtained without even solving the fluid dynamics part of the equations.

In Sharma *et al.*[27], formation of oil droplets in a water medium is numerically investigated via COMSOL. In the modeled system, both previously mentioned liquids are pumped into a T-shaped microchannel—where water is the continuous phase and oil is the dispersed phase—and subjected to an external AC electric field. It had previously been found that droplets can form inside a pressure-driven flow in a microchannel, only within a certain range of flow ratios of the incoming phases and the purpose of this study is to find out if it is possible to widen this range. It is shown that water and oil form a flat interface when oil enters the microchannel horizontally at a certain flow ratio and it is possible to deflect this interface and induce droplet formation by subjecting the system to a normal AC electric field. When the incoming phases are purely dielectric, the electric field induces droplet formation however, decreasing the frequency of the applied voltage seems to have no effect on the droplet size and the frequency of droplet formation remains unchanged. Conversely,

when the incoming phases are both weakly conducting, the frequency of the applied voltage reduces droplet size and increases the frequency of droplet formation. It has been shown that the interfacial contact length (L_i), which is the product of the number of droplets and the perimeter of each droplet, and the frequency of droplet formation (D_f) decrease when the frequency of the applied voltage (f) is increased. In contrast, both quantities have a positive correlation with the conductivity ratio ($\sigma_r = \sigma_{oil}/\sigma_{water}$) of the liquids. One more finding in this paper is that the shape of the wave generated by the AC electric source effects the diameter of the droplets (d_d) and the D_f. i.e. When two different waves are generated with the same amplitude and frequency but different shapes, one sinusoidal and the other triangular, the former induces big droplets at a lower rate and the latter creates smaller ones at a higher rate.

2.3. Direction of the Applied Electric Field

The stability of the flat interface between two immiscible liquids in the presence of an external electric field, either normal or parallel to the said interface, is investigated in the work by Eribol and Uguz[28]. The effect of an electric field on the interface between both two perfect dielectric liquids and two leaky dielectric liquids is addressed in the work. It is concluded that the direction of the applied electric field can have varying effects on the system. Namely, the interface between two leaky dielectric liquids can remain stable up to a certain value of the applied electric field when the said electric field is normal to the interface and after this point the interface starts to deform. However, when the applied electric field is parallel to the interface, it cannot cause enough disturbance in the system to cause deformation of the interface for certain values of the viscosity ratio, flow rate ratio and total flow rate of the incoming phases.

Uguz *et al.*[26] showed, through a linear stability analysis, that the direction of the applied electric field has varying effects on the stable interface between two immiscible, leaky dielectric liquids. The numerical study suggests that electric fields (normal or parallel to the interface) can have either a stabilizing or a destabilizing effect of the interface depending on the conductivity and permittivity ratios of the liquids used in the system. It was concluded that a normal electric field has a destabilizing effect within wider ranges of the said ratios than a parallel electric field.

In Haiwang *et al.*[29], electrohydrodynamic and shear-stress instability of the interface between two immiscible liquids—aqueous $NaHCO_3$ as the conducting liquid and silicone oil as the non-conducting liquid—in a microchannel is investigated analytically and experimentally. It has been propounded in the paper that an electric field applied tangentially to the interface, can have a stabilizing or destabilizing effect depending on the viscosity ratio of the liquids and the direction of the electric field and such behavior can be predicted via an analytical model. The results of the experiments disclose a stabilizing effect of the tangential electric field when it is applied in the direction of the pressure-driven flow (the positive direction). In this scenario, the growth rate of the disturbance is negative for all wave numbers, indicating a stable interface. In addition, electric fields in the positive direction favor non-conducting to conducting liquid thickness ratio due to electroosmotic effects, i.e. as the magnitude of the applied electric field increases so does the thickness ratio. On the other hand, when the electric field is applied in the negative direction (the direction opposite to that of the pressure-driven flow), the interface managed to remain stable only up to a certain threshold magnitude of the electric field, which is referred to as "the critical electric field" and above which the interface becomes unstable and turns into perturbed ripple waves. It has been observed that increasing the viscosity of the conducting phase has a stabilizing effect on the interface for each setup. It has also been found that increasing electric field strength (positive when applied in the flow direction and negative otherwise) have a dwindling effect on growth rate and the same effect is observed for the channel width and the total flow rate; i.e. an increase in any of the said parameters results in a more stable interface. Finally, it has been reported that their theoretical model is able to predict the experiments with up to 39% error.

In Haiwang *et al.*[30], interfacial instability of the interface between two liquids—one aqueous $NaHCO_3$ solution with high electrical mobility and the other silicone oil with low electric mobility—in the presence of a normal electric field is analytically and experimentally investigated and the results are compared. In the experimental setup, these immiscible liquids are pumped into a microchannel and a flat interface between them is observed. After the formation of the interface, the system is subjected to an electric field that is normal to the interface, and the response of the system is recorded. For each configuration of the setup (i.e. varying viscosities of the conducting phase, total flow rates and channel

widths), there is a threshold value of the electric field—referred to as the “critical electric field”—after which the interface starts to destabilize, and the paper focuses mainly what happens after this point. The quantitative analyses reported in the paper show that there is a positive correlation between the growth rate of the disturbance and the applied electric field, i.e. when the applied electric field increases, so does the growth rate for a fixed viscosity of the conducting phase. The same pattern is observed for the growth rate versus the channel width as well. It turns out that channel width, along with applied voltage, has a destabilizing effect on the interface. As opposed to the previously mentioned parameters, total flow rate plays a different role in the interfacial stability. Increasing the total flow rate evidently has a stabilizing effect on the interface. Finally, the theoretical model proposed in the article proved to be effective in predicting the interface response to the normal electric field.

2.4. Direct Current and Alternating Current

Gamphire and Thaokar[31] showed that the frequency of the AC electric field has a significant effect on the instability of the interface between two immiscible, leaky dielectric liquids via linear instability and Floquet analyses. They observed that implementation of an AC electric field can result in stabilization of the interface as opposed to that of a DC electric field. The effect of an AC electric field was investigated at the low and high frequency limits and it was concluded that the growth rate of the instabilities of the interface can be manipulated to remain between that of perfect dielectrics in the presence of a low frequency AC field and that of leaky dielectrics in the presence of a high frequency AC field. In addition, an AC electric field can cause disturbances and, consequently, cause deformation of the interface, at the zero-frequency limit.

The effect of an AC electric field on both the size and shape of the pillars formed, as a result of destabilization of the interface between two thin layers of liquids that are immiscible and leaky dielectric, is investigated by Roberts and Kumar[32]. The work required the implementation of the leaky dielectric model since the perfect dielectric model resulted in a vague distinction, if at all, between a DC electric field and an AC one. The results of the numerical analysis point toward a better control over the accumulation of free charges at the interface and over pillar formation.

2.5. Droplet Formation

Droplet microfluidics focuses on control over the generation of droplets, frequency of generation, droplet size and utilization of the said droplets in various applications. This process requires the presence of two immiscible liquids flowing in a microchannel since, by definition, one of the said phases (the dispersed phase) needs to take the form of a droplet of finite volume encapsulated by the other phase (the continuous phase) in a controlled fashion. The formation of these droplets is caused by the destabilization and deformation of the interface between the said liquids and eventually resulting in capture of the dispersed phase within the continuous phase[33].

Generation of droplets in such systems, the size of the droplets and the frequency of generation can be controlled and manipulated via certain methods that can be categorized mainly as passive and active methods[34]. The passive methods rely on flow patterns and complex geometries of the microchannels such as co-flowing[35], T-junction[36] and flow focusing[16] to cause destabilization of the interface between the phases and droplet formation. The active methods, on the other hand, rely on external disturbances such as thermal actuation[37], a magnetic field[38] or an electric field[24] to cause the said phenomenon.

In the case of application of an electric field there are certain parameters, that can be set as properties of the electric field, in order to facilitate a desired droplet generation. These parameters include the applied voltage and the distance between the electrodes[28] in the case of a DC electric field; the frequency[31] and waveform in the case of an AC electric field. Generation of monodisperse droplets from two immiscible leaky dielectric liquids flowing in a microchannel was studied by different groups. Ozen *et. al*[17], proposed the application of a DC electric field normal to the stable interface between two Newtonian liquids and were able to generate droplets that are 0.4 to 0.6 μL in size via an applied voltage of 200 to 600 V.

3. EXPERIMENTAL WORK

3.1. Chemicals

In the experiments, ethylene glycol and 50 cSt silicone oil are used as Newtonian liquids. These chemicals were chosen (Table 3.1) based on their non-toxic, non-volatile natures along with the fact that they are immiscible and non-corrosive on PMMA surfaces that are used as the top and bottom plates of the microchannels.

For the Newtonian/non-Newtonian phase systems, silicone oil is utilized once again as the dispersed phase and a solution of xanthan gum and aqueous glycerol is chosen as the continuous phase. These chemicals are chosen due to their non-hazardous natures. An aqueous solution (85% by volume) of glycerol is used to overcome the difficulty of pumping pure glycerol, which has a high viscosity, into the microchannels. Xanthan gum is added, in small amounts (250 ppm), to aqueous glycerol to give the solution a non-Newtonian, shear-thinning behavior[39].

Table 3.1. Physical properties of the chemicals used in the experiments.

Chemical	Brand / Vendor	Density, ρ (g/cm^3)	Kinematic Viscosity, ν (cSt)	Conductivity, σ (S/m)	Relative Permittivity, ε
Silicone Oil (50 cSt)	Sigma - Aldrich	0.96	50	1.0E-13	2.72
Ethylene Glycol	ISOLAB Chemicals	1.11	15.0	1.1E-04	37.7
Glycerol (85%)	ISOLAB Chemicals	1.23	77.6	3.0E-03	-
Xanthan Gum	TEKKİM Chemicals	-	-	-	-

3.2. Experimental Setup

All of the experiments were carried out in the same experimental setup which consists of a Nikon Eclipse LV100POL optical microscope (Nikon Instruments Europe B.V.) ❶, a Dual Drive System 33 syringe pump (Harvard Apparatus, USA) ❷, a Rohde and Schwarz HMF2525 25MHz function generator (Rohde & Schwarz Inc., U.S.A.) ❸, a Rohde & Schwarz HMO1002 Series oscilloscope (Rohde & Schwarz Inc., U.S.A.) ❹, a Fastec InLine high-speed camera (Fastec Imaging, USA) ❺, a TREK 5/80 high voltage amplifier (TREK Inc., U.S.A.) ❻, an assembled desktop computer ❼, two 20 mL plastic syringes, poly ethylene tubing (Scientific Commodities Inc., USA) with an inner diameter of 0.72 mm and an outer diameter of 1.22 mm and green 21G (outer diameter of 0.81 mm) needles and a handmade microchannel ❽. A photo and a schematic view of the experimental setup can be seen in Figure 3.1.

The microchannel is placed on a microscope stage, illuminated from below and viewed from above. A Nikon CFI Plan Achromat 2x objective is chosen for a good observation since its field of view, which is 12.50 mm, can cover a sufficiently large portion of the microchannel at a time (Figure 3.2). The visual output is sent to the desktop via high-speed camera where it is processed by the computer software FIMS DEMO 3.0.

Meanwhile, the liquids required for the generation of a stable interface are pumped into the microchannel via a syringe pump (Figure 3.3), which then pass through polyethylene tubing and flow into the microchannel whose electrodes are connected to the amplifier which takes its input from the function generator and is monitored with the oscilloscope.

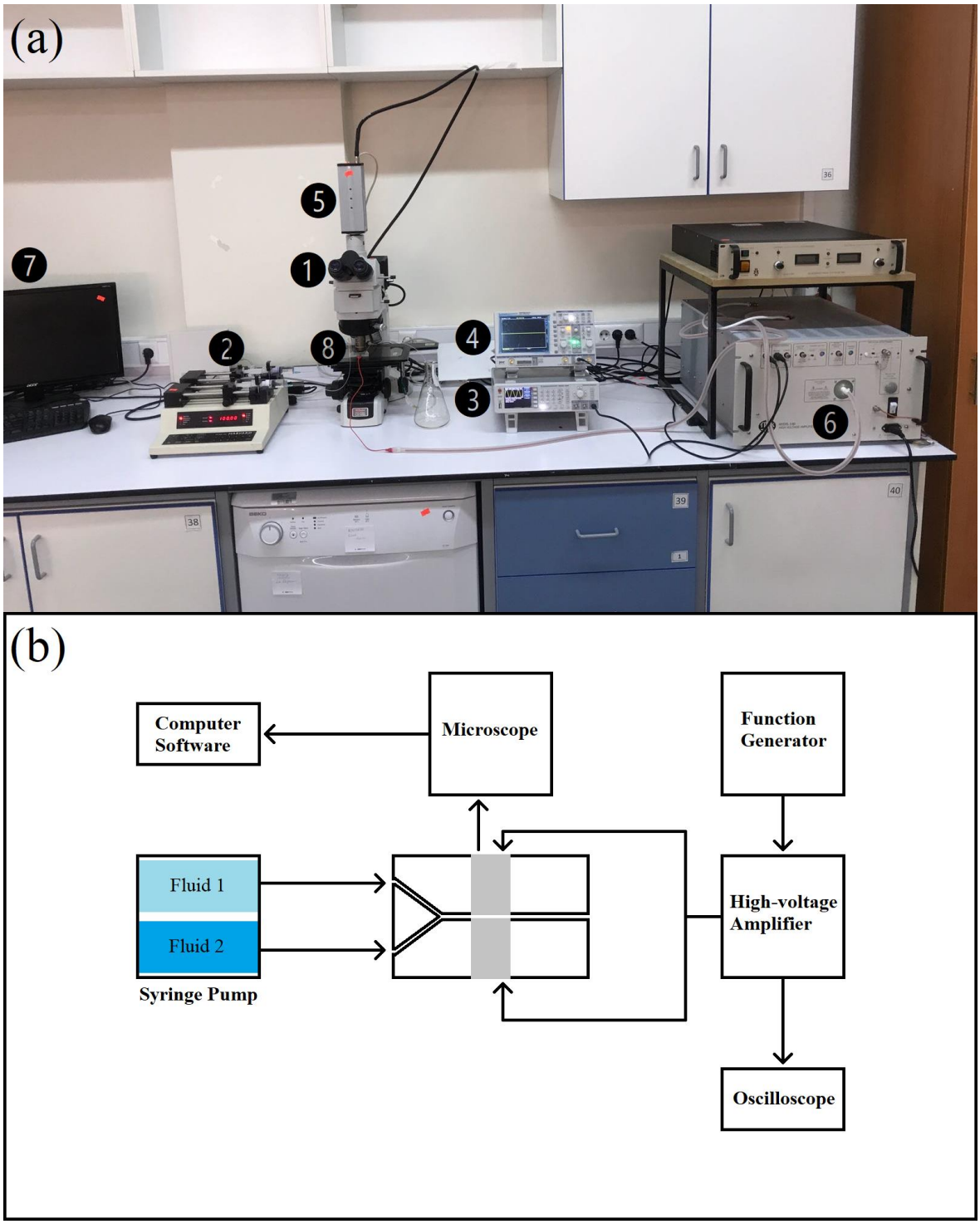

Figure 3.1. (a) The experimental setup and (b) a schematic view of the experimental setup.

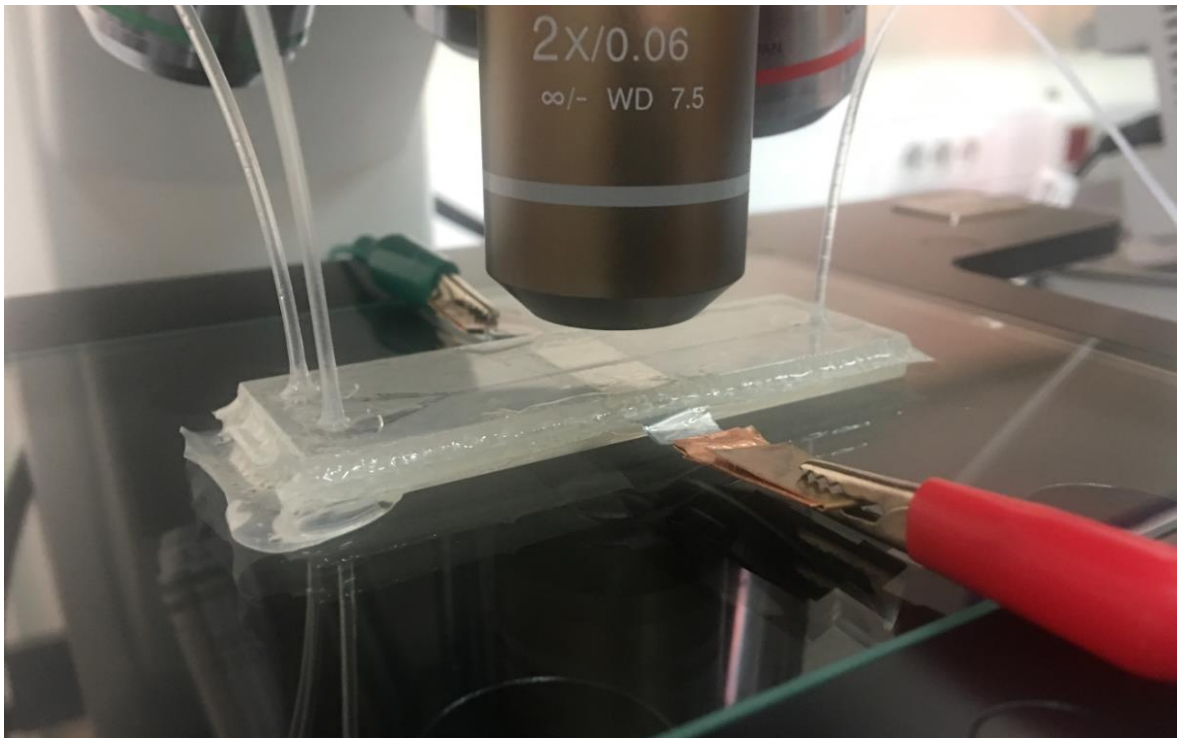

Figure 3.2. A microchannel under the 2x objective.

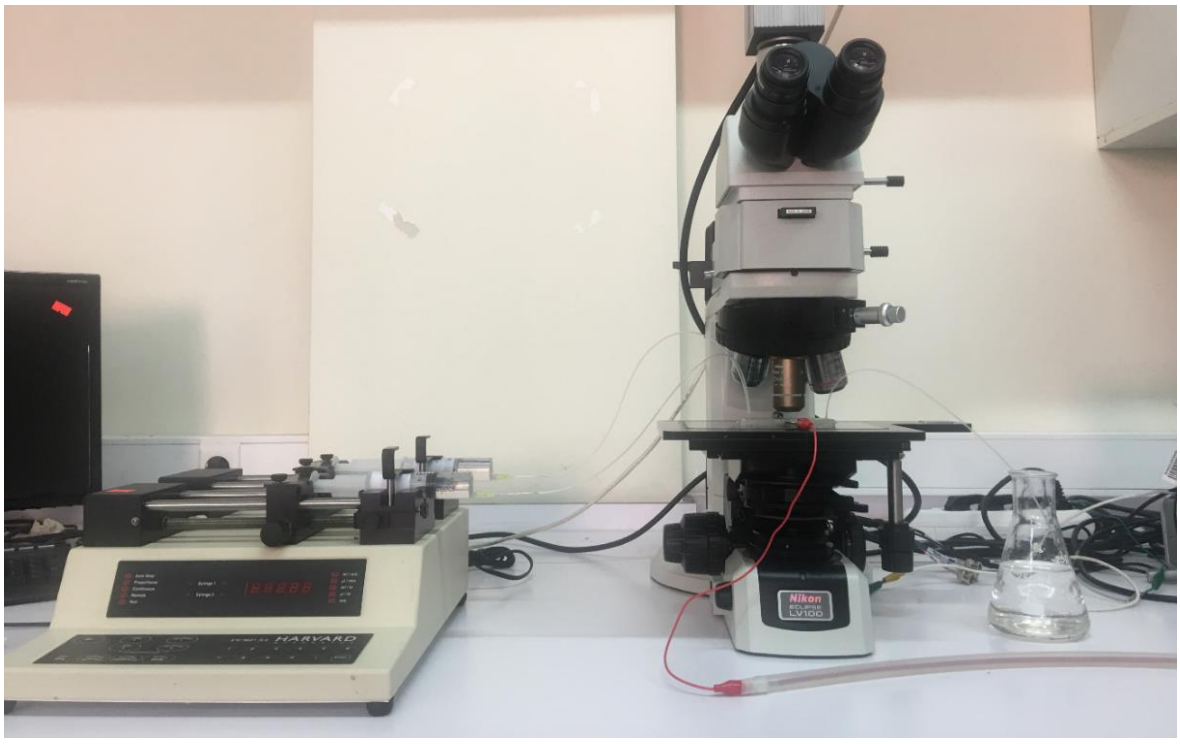

Figure 3.3. Syringe pump, pumping liquids into the microchannel.

3.3. Microchannel Design and Fabrication

An acetate sheet is laser-cut into rectangular parts that are 5 cm in length and 1.2 cm in width. The acetate pieces, then, are wiped clean with ethanol to prevent debris from entering the channel and blocking and/or hindering the flow of the liquids. A piece of aluminum tape (AKBANT Folyo Bant, adhesive only on one side) is cut into strips of 1 or 2 cm width and of whatever length, which is also the electrode length, is needed. The aluminum strip is aligned so that it is in the middle of the small acetate sheet and the fringes of the aluminum strip make a 90° angle with the long side of it. The aluminum strip is tightly wrapped around the acetate sheet along its width for the making of the electrodes and is later checked for air bubbles that might cause imperfections inside the channel. At this point, the aluminum strip covers 3 sides of the acetate sheet—it runs along the width on top, goes down along the depth and runs back along the with at the bottom. The depth of the acetate is to be the depth of the electrode and the width of the aluminum strip, its length. Two pieces of transparent duct tape (MAS Invisible tape), then, wrapped around the acetate sheet at the two edges of the aluminum strip for height adjustment. This whole procedure is done under a microscope so that there are as little gaps between the aluminum strip and the duct tapes and as fewer imperfections on the channel side of the electrode piece as possible. A photograph of the electrode piece is given in Figure 3.4.

In the next step, both sides of the electrode piece are covered with double sided tape (Pattex, Transparent double-sided tape) to make an assembled piece (Figure 3.5) so that it can hold the electrode pieces and the top and bottom PMMA (PIA Acrylic, 3 mm thick cast plexiglass) plates together. The long side of the double-sided tape is properly aligned with that of the electrode piece so that there are no indentations on the microchannel walls. Next, the assembled pieces are aligned so that their aluminum strips exactly face each other, and they are cut on one side diagonally to make a T-junction for the incoming liquids.

One of the assembled pieces is fixed on the top PMMA plate that has two inlet holes and an outlet hole, making sure that the assembled piece does not block any of the said holes. The second assembled piece, then, is fixed on the top PMMA plate, making sure that its aluminum strip is facing that of the first assembled piece, that it is not blocking any inlet or

outlet holes and that it is properly distanced from the first assembled piece with the help of a microscope slide which has a thickness of roughly 1.10 mm.

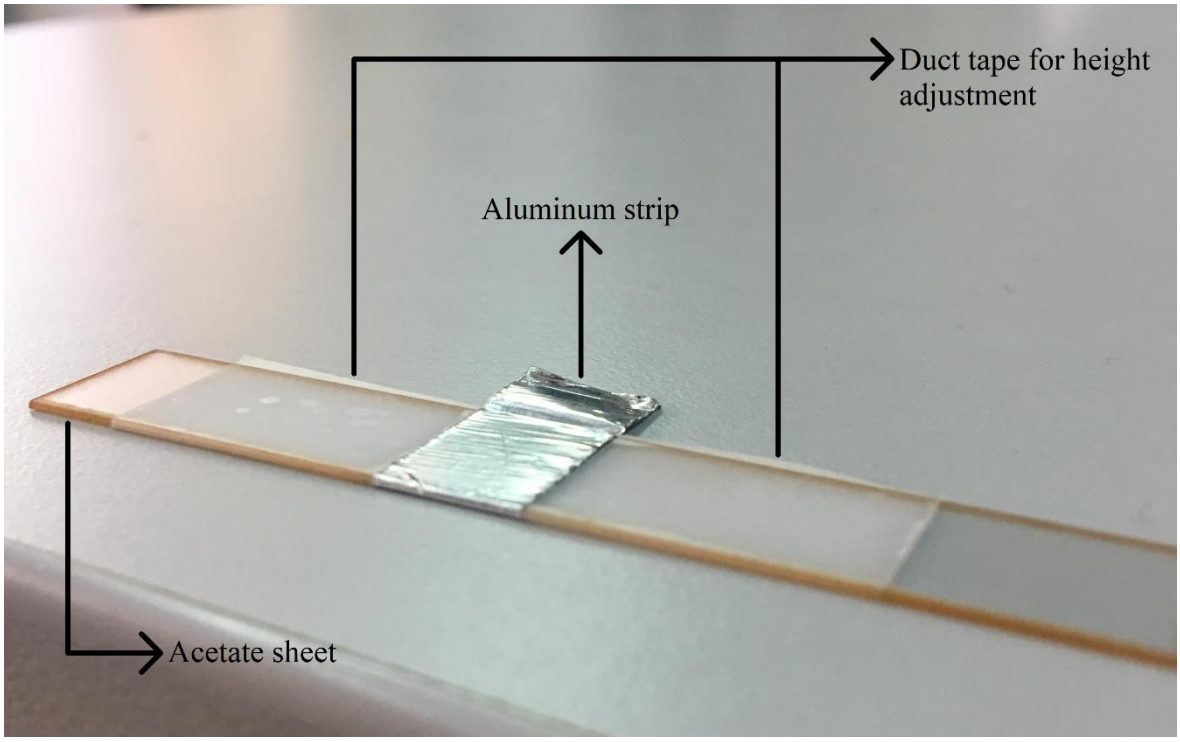

Figure 3.4. Electrode piece.

In the final step, the bottom PMMA plate is placed on top and pressure is applied on the microchannel assembly to ensure that both PMMA plates are in good contact with the adhesive of the double-sided tapes to avoid leakages. Polyethylene tubing are cut in desired lengths and are inserted into the microchannel through the inlet and outlet holes and later sealed with glue. In addition to applying pressure, a layer of glue can be smeared around the microchannel where the double-sided tapes meet the PMMA plates to lessen the probability of a leakage. Since the fringes of the aluminum strips can be torn or damaged easily, they are attached to slim, bendable pieces of copper with the help of double-sided copper tape.

Figure 3.5. Assembled piece.

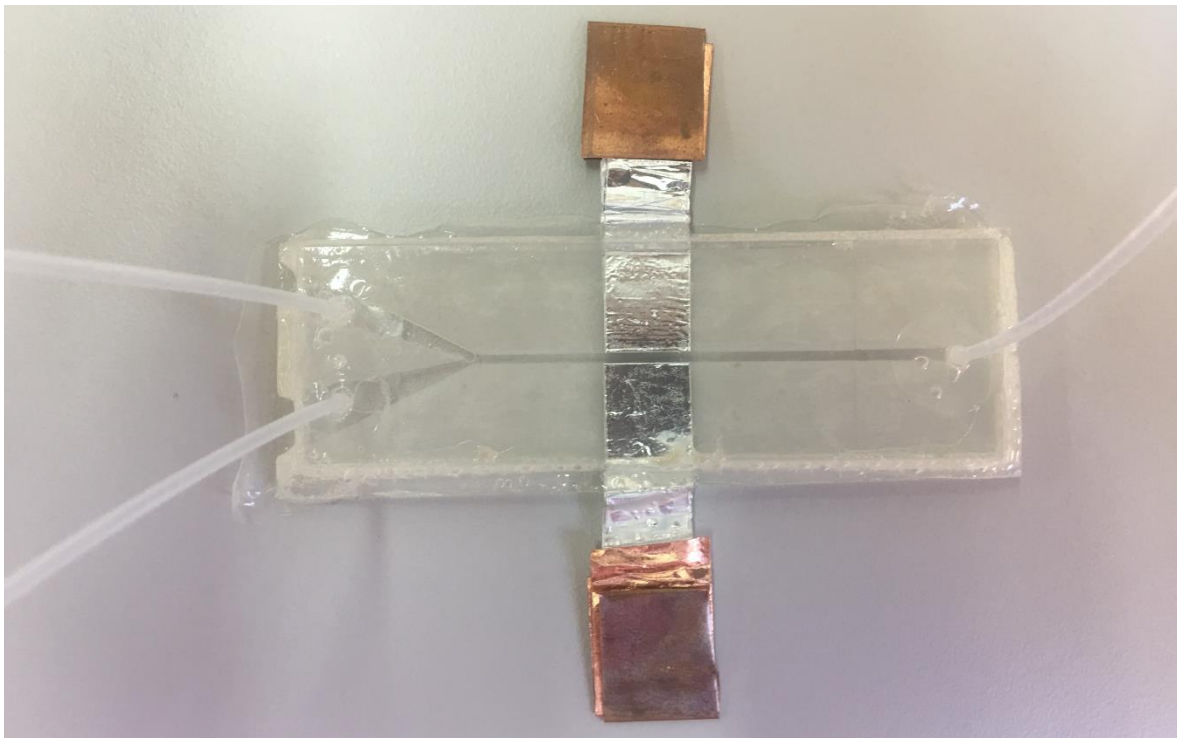

Figure 3.6. Top view of a microchannel.

3.4. Procedure of the Experiment

The free ends of the inlet tubes are attached to the needles which are attached to the syringes. Both liquids are pumped into the microchannel via the syringe pump. The desired volumetric flow rates (Q_1, which is the oil phase and Q_2, which is the aqueous phase) can be obtained by entering the numbers (in μL/min) to the syringe pump. The electrodes of the channel are connected to the high-voltage amplifier (initially turned off). As flow develops inside the microchannel, the system is left to rest for a stable interface to form between the two immiscible liquids. This process is monitored via the slow-motion camera. After a stable flat interface is obtained, its distance to the upper wall (when viewed from above, Figure 3.6) of the microchannel is measured and recorded as H_1. This number, then, is subtracted from the whole thickness of the microchannel, and the result is recorded as H_2. The ratio of these two numbers (H_1 / H_2) gives the thickness ratio (H_r). Then, the function generator is turned on along with the oscilloscope and the high-voltage amplifier. The voltage applied is raised slowly, by increments of 10 V at each step. It is essential to give the system enough time to stabilize or destabilize after each 10 V increase. At a certain value of the applied electric field, the interface becomes unstable and hits against the upper wall of the microchannel (the details will be provided in the Results and Discussion part). This voltage value is read from both the function generator and the oscilloscope and recorded as the critical voltage (V_c). It should be noted that this is peak to peak voltage. This procedure is repeated for both parts of the experimental work—the first part involves experiments with two Newtonian liquids (N-N system) and the second part, with a Newtonian and a non-Newtonian liquid (N-nN system).

As the interface periodically hits against the wall of the microchannel, microdroplets are formed. The formation of the microdroplets and their sizes are examined for the N-nN system. One of the observations made is that a N-nN interface does not immediately form droplets when it reaches its critical voltage. Instead, the interface touches the wall and remains bent/distorted, taking a new stable form. For the N-nN systems, the voltage applied is raised again above their critical voltages, only this time by increments of 100 V to observe periodic formation of constant size droplets. The formation and motion of the formed droplets are recorded (in 60 frames per second) via the software FIMS DEMO 3.0 (Figure 3.7). The recorded frames are used to measure the surface area of each droplet formed via

the software ImageJ (Figure 3.8). As the droplets are in the form of slugs, finally the measured surface area of the droplets is multiplied with the depth of the channel, which yields the volume of the droplets.

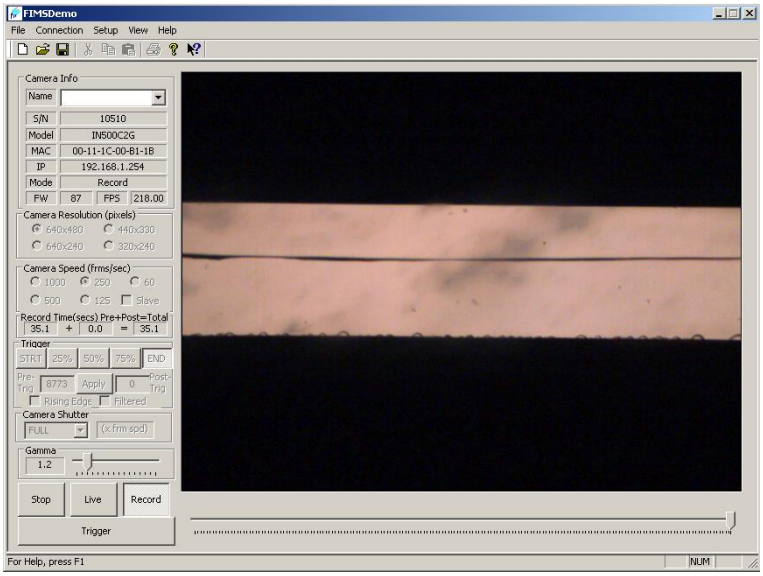

Figure 3.7. Screenshot of FIMS DEMO 3.0 software interface.

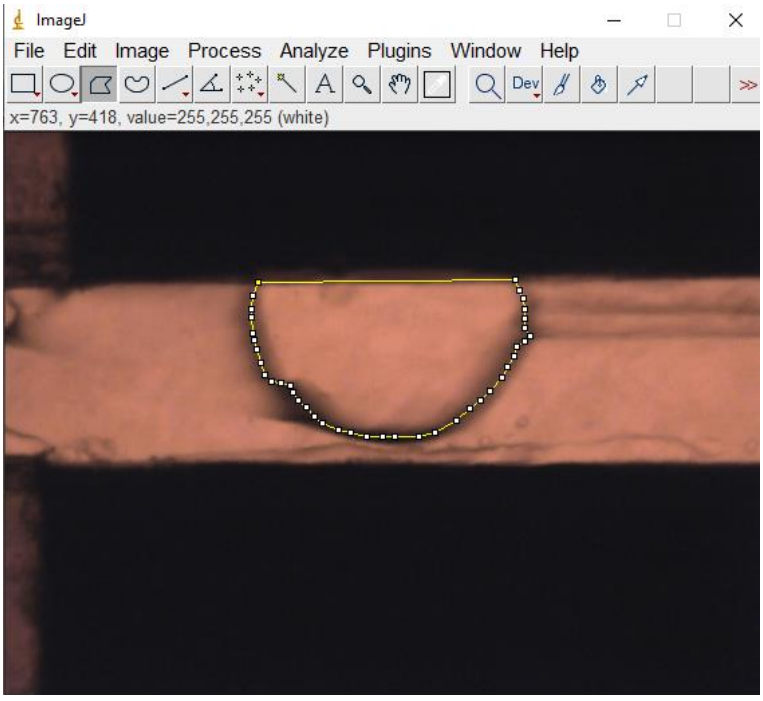

Figure 3.8. Screenshot of ImageJ software interface.

3.5. The Default, Controlled and Measured Parameters

In order to conduct these experiments in a controlled manner, a default configuration was chosen. The main difference between the aforementioned stages is the choice of the continuous phase. The features of the default configurations are shown in Tables 3.2 and 3.3.

Table 3.2. The Newtonian / Newtonian system default configuration.

Fluid 1	: Silicone oil (50 cSt)
Fluid 2	: Ethylene glycol
Channel Depth (mm)	: 0.55 (± 0.17%)
Channel Width (mm)	: 1.10
Electrode Length (mm)	: 10
Q_T (μL/min)	: 180
Electric Field Frequency (kHz)	: 5
Waveform	: Sine

At this configuration, varying values of Q_1 and Q_2 are used as input and the resulting thickness ratios and critical voltages are measured. For comparison, the electric field frequency is chosen as 0.5 kHz and the electrode length is chosen as 20 mm in different sets, for the N-N system.

Table 3.3. The Newtonian / non-Newtonian system default configuration.

Fluid 1	: Silicone oil (50 cSt)
Fluid 2	: Xanthan gum / Aqueous glycerol solution (250ppm)
Channel Depth (mm)	: 0.36 (± 2.8%)
Channel Width (mm)	: 1.10
Electrode Length (mm)	: 10
Q_T (μL/min)	: 180
Electric Field Frequency (kHz)	: 5
Waveform	: Sine

For the nN-N system, the critical voltage is measured for different thickness ratios. In addition, droplet sizes at voltages above the critical value are analyzed at two different thickness ratios, namely at 0.60/3.6 and 0.9/3.3.

4. RESULTS AND DISCUSSION

In this section, the input values and the measured data are presented. The input values that are kept constant and/or controlled are Fluid 1 which is silicone oil with a kinematic viscosity of 50 cSt, Fluid 2 which is ethylene glycol (EG) for the N-N system; 250 ppm xanthan gum in 85% aqueous glycerol (XG/AGl) solution for the N-nN system, channel depth (0.55 mm for the N-N system; 0.36 mm for the N-nN system), channel width (1.10 mm), electrode length (10 and 20 mm for the N-N system; 10 mm for the N-nN system), total flow rate which is the sum of the volumetric flow rates of the incoming liquids (Q_T = 180 μL), electric field frequency (0.5 and 5 kHz for the N-N system; 5 kHz for the N-nN system) and waveform (sine).

The range of Q_r is chosen so that the stable interface between the liquids is always positioned at or above half of the channel width, that is, H_r is always equal to or less than 1. At H_r values above 1, it is observed that the critical voltage to destabilize the interface is too high and can compromise the integrity of the microchannels as observed in Figure 4.1c and 4.1d. For the N-N system, the flow rate of silicone oil (Q_1) is started at 50 μL/min and lowered, by increments of 5 μL/min, down to 15 μL/min. This is the point where the last stable interface is achieved, after which the flow started passively generating droplets. The flow rate of ethylene glycol (Q_2), in return, is started at 130 μL/min and increased, by increments of 5 μL/min, up to 165 μL/min to maintain a total flow rate of 180 μL/min at each run. The resulting thickness ratios are measured via the FIMS DEMO 3.0 software and turn out to be within the range 0.28-1.00. Another measured parameter for the N-N systems is V_c which is the peak-to-peak values of the critical voltage and is measured in kV. These values range from 0.68 to 2.18 kV.

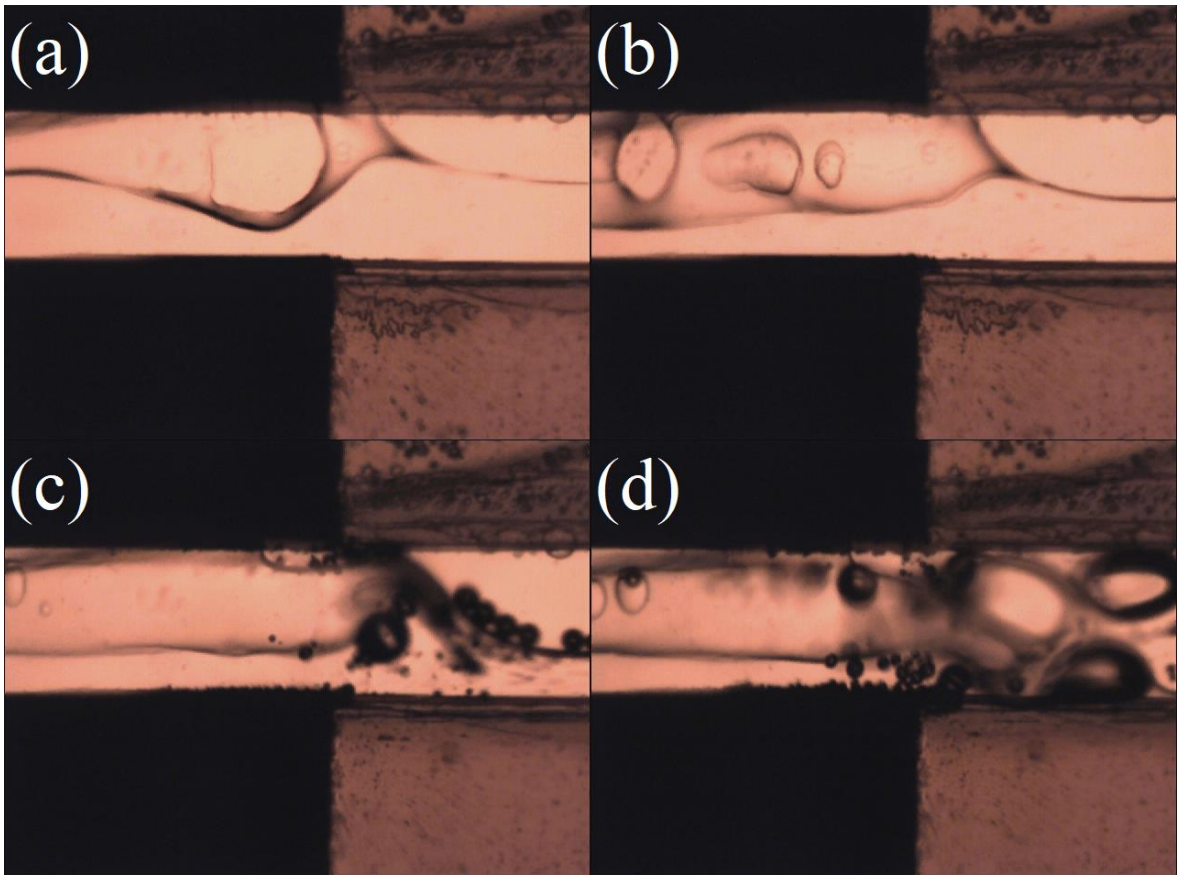

Figure 4.1. Effect of high voltage on the microchannel. Top: silicone oil at 90 μL/min, bottom ethylene glycol at 90 μL/min. (a) The interface hits the electrode, (b) wetting and droplet formation occurs, (c) bubbles start to form, (d) the microchannel is disintegrating.

For the N-nN system, the initial flow rate of silicone oil is chosen as 105 μL/min and that of the xanthan gum/aqueous glycerol solution (XG/AGl) as 75 μL/min since these flow rates result in an H_r value of 1.00. Q_1 values of the N-nN system is reduced (and in return, Q_2 values raised) by 10 μL/min for the second and third steps which yielded H_r values of 0.64 and 0.52. At this point, it is observed that even though the interface between the liquids can be destabilized at high voltages, droplets cannot be generated without increasing the applied voltage above safe values (without damaging the microchannel). So, in the following steps, Q_r (and therefore H_r) are reduced in a non-uniform fashion until periodic droplet generation is attained at safe voltages. For the N-nN system, V_c values range from 0.54 to 2.73 kV.

It is observed that droplet formation processes are significantly different in the N-N and the N-nN systems. i.e., the Newtonian liquids seem to periodically generate droplets of the dispersed phase at their V_c—the moment the interface starts flapping against the upper (in top-down view) wall of the microchannel (Figure 4.2). However, the interface between the Newtonian and non-Newtonian liquids, when the V_c is reached, hits the upper wall and takes another stable form, not generating droplets (Figure 4.3). The applied voltage must be increased further above the V_c in order to achieve periodic droplet formation. Formation of the droplets is examined for two H_r values of the N-nN system; namely, 0.17 and 0.27. The $H_r = 0.17$ system (with $V_c = 0.56$ kV) generated droplets that are 0.417 to 0.516 μL in volume within an applied voltage range of 0.96 to 3.06 kV where the $H_r = 0.27$ system (with $V_c = 1.00$ kV) was able to produce droplets that are 0.353 to 1.499 μL in volume within an applied voltage range of 2.13 to 3.53 kV.

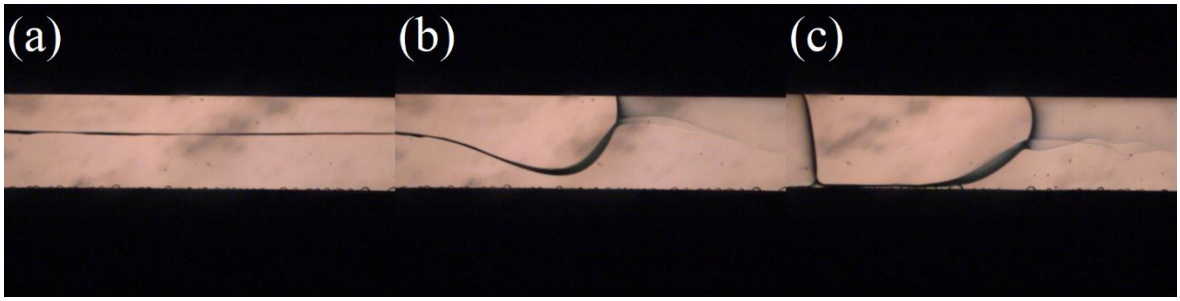

Figure 4.2. Droplet formation in the N-N system. (a) flat interface, (b) interface hitting the electrode wall, (c) droplet formation at V_c.

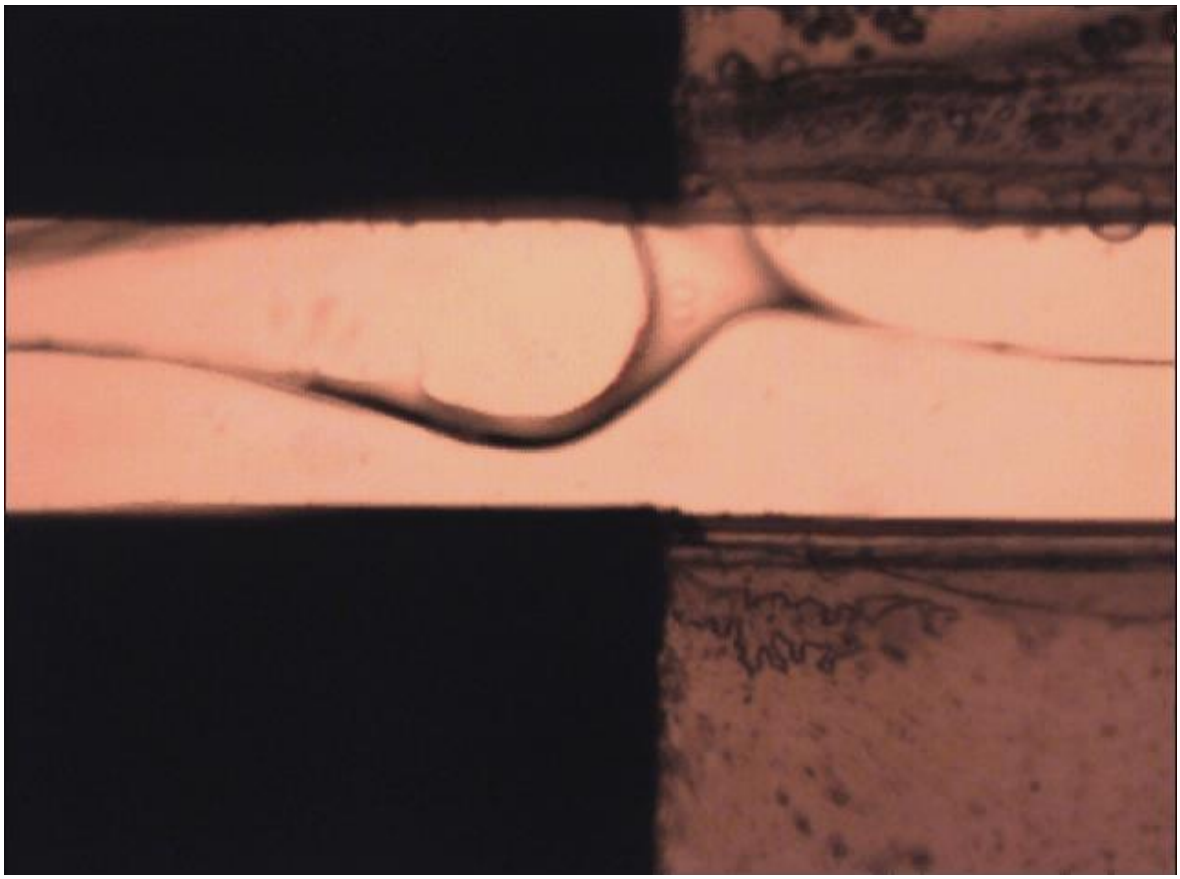

Figure 4.3. The Newtonian/non-Newtonian interface hitting the wall and taking another stable form.

4.1. Electrohydrodynamic Instability for the Newtonian/Newtonian System

In this section, the effect of the flow rate ratio on the thickness ratio and the effect of the thickness ratio on the critical voltage are shown and discussed. Additionally, the effect of the electric field frequency (f) and the electrode length on the critical voltage are presented.

4.1.1. Effect of Volumetric Flow Rate Ratio on Thickness Ratio

The H_r vs. Q_r data is plotted in Figure 4.4. As expected, an increase in Q_r causes an increase in H_r. That is, when the relative amount of Fluid 1 being pumped into the channel increases, so does the amount of volume it occupies inside the microchannel.

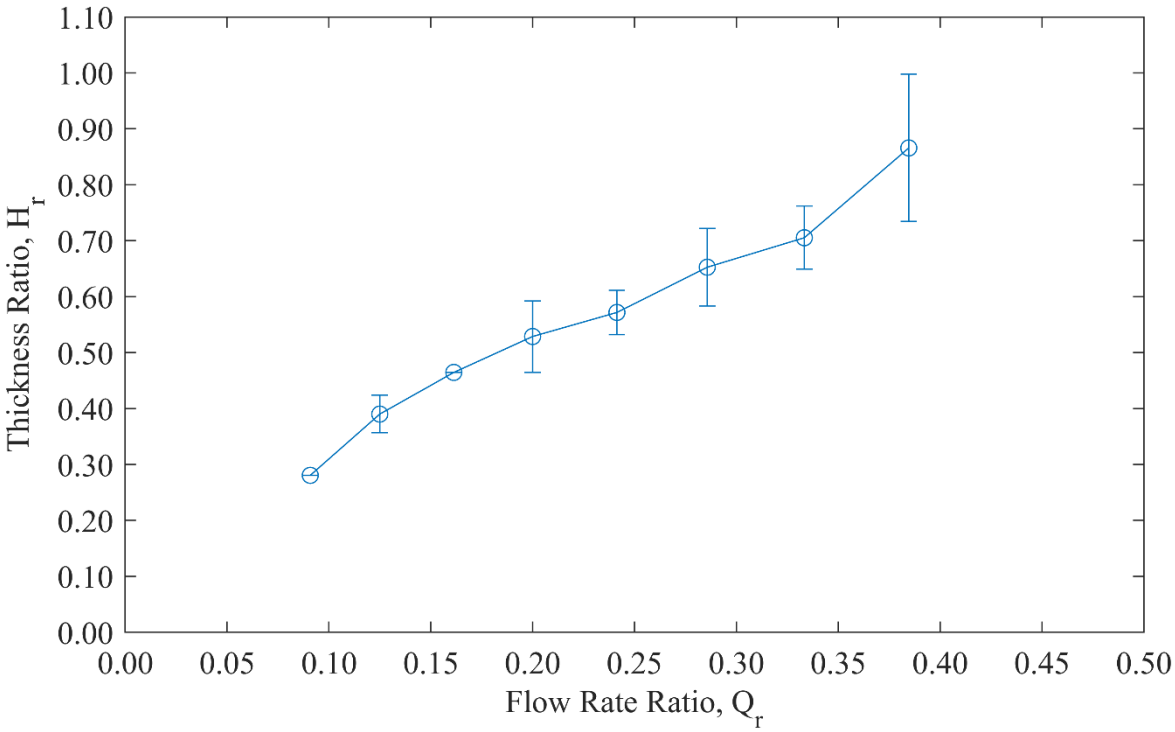

Figure 4.4. Average thickness ratio vs. flow rate ratio for the N-N system.

4.1.2. Effect of Thickness Ratio on Critical Voltage

In the following figures (4.5, 4.6 and 4.7), the V_c vs. H_r data are plotted. There is a positive correlation between these parameters in all configurations of the N-N system, which suggests that the magnitude of the applied electric field to destabilize the flat interface increases as the thickness of the dispersed phase increases. This curve should theoretically approach the point (0, 0) since it becomes easier to destabilize the interface as the thickness of the dispersed phase decreases and the flat interface approaches the upper wall of the microchannel. In fact, the smallest value of H_r was recorded as 0.28 for the N-N system and below this point a stable interface could not be achieved. The interface started flapping against the upper wall even in the absence of an applied electric field (passive droplet formation). In addition, the critical voltage seems to be increasing at decelerating rates (Figure 4.5), which is in agreement with the work of Altundemir *et al.*[21].

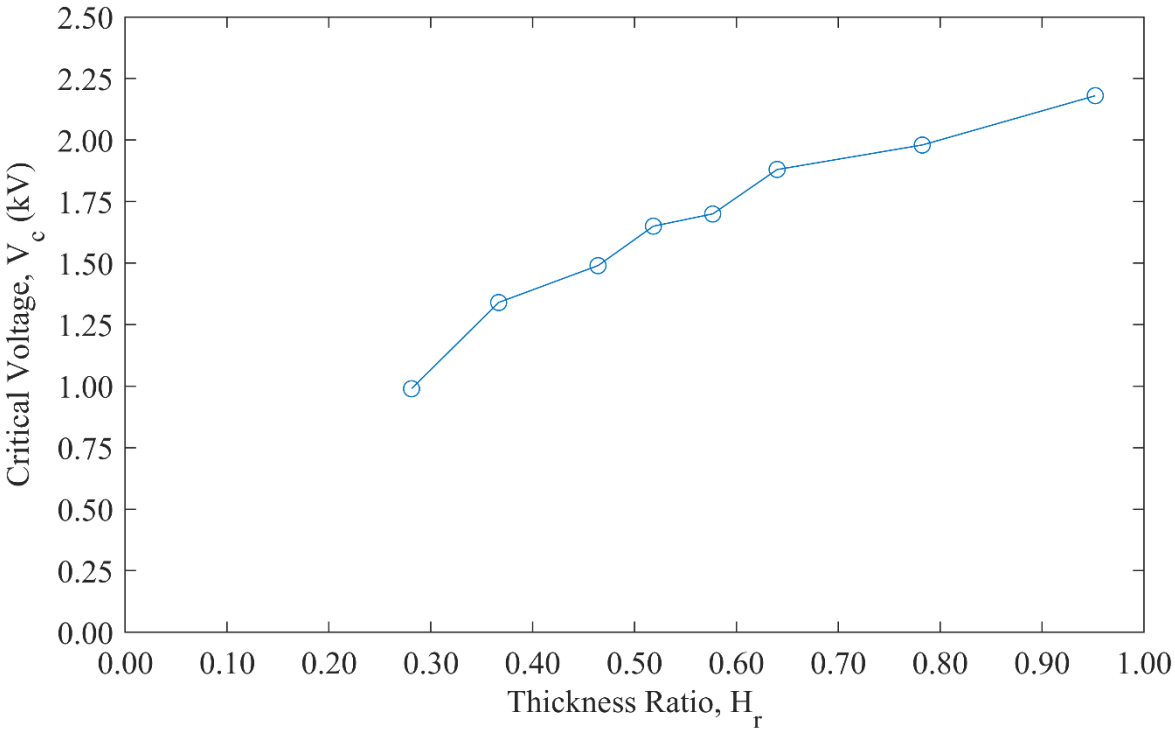

Figure 4.5. Critical voltage vs. thickness ratio for the default configuration of the N-N system.

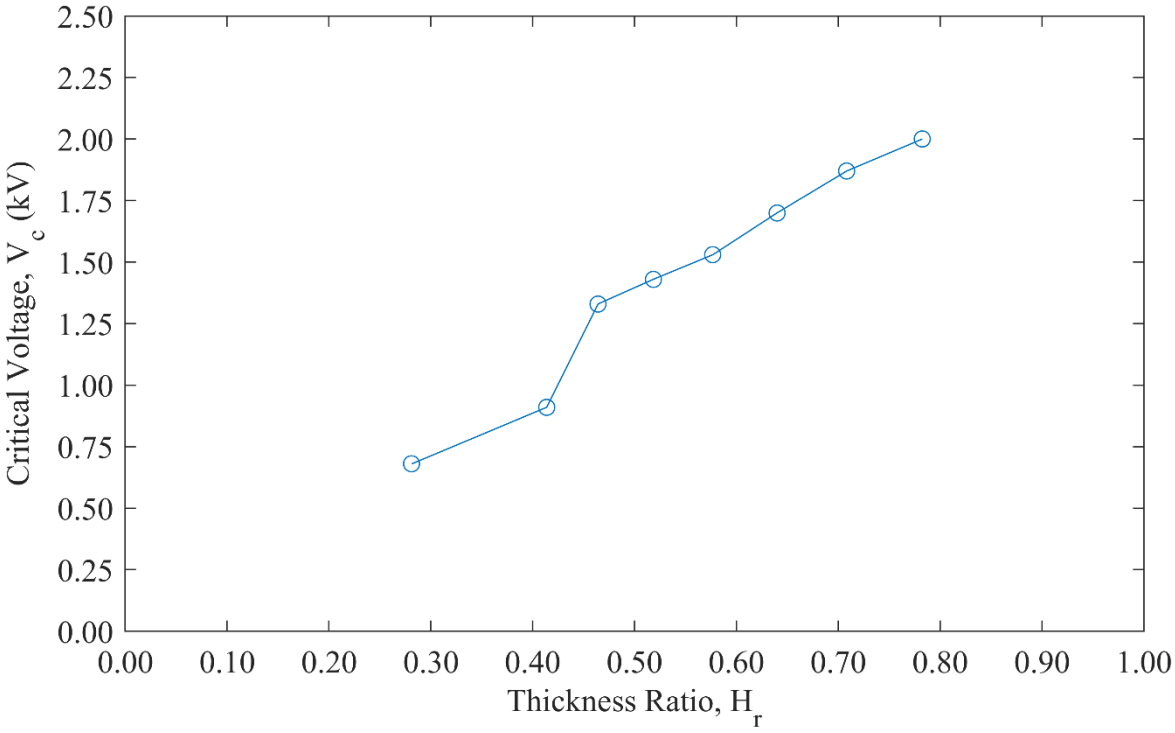

Figure 4.6. Critical voltage vs. thickness ratio for f = 0.5 kHz in the N-N system.

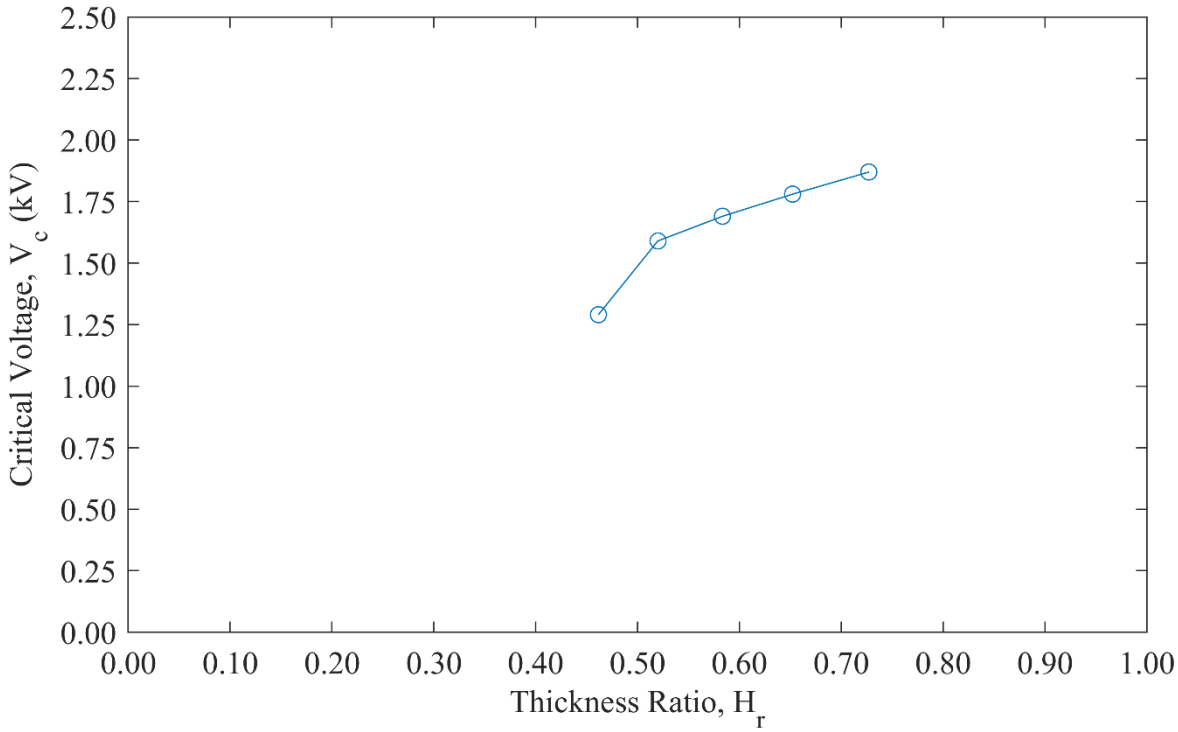

Figure 4.7. Critical voltage vs. thickness ratio for L_e = 20 mm in the N-N system.

4.1.3. Effect of Electrode Length on Critical Voltage

In Figure 4.8, the V_c vs H_r curves for two different electrode lengths, 10 mm and 20 mm, are compared. The V_c corresponding to the 10 mm electrode is at least 93 V more than the V_c for the 20 mm electrode microchannel. Longer electrode lengths expose greater portions of the interface to the electric field, which could explain the decrease in V_c when the electrode length is 20 mm.

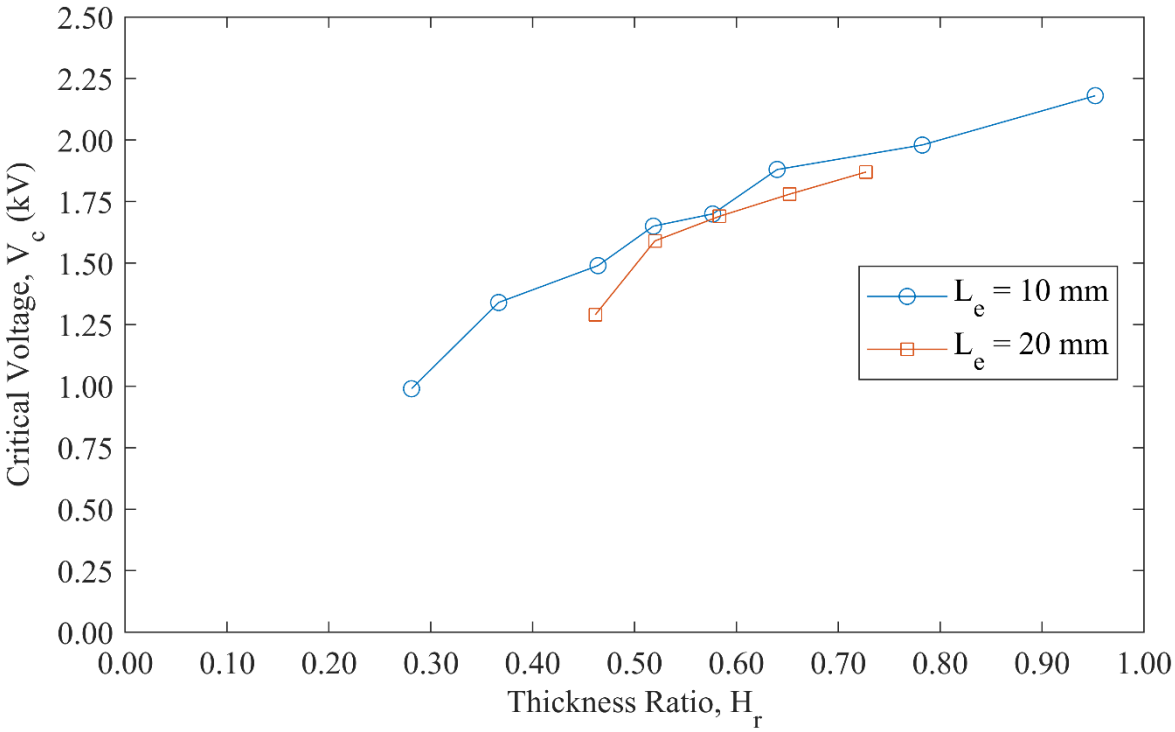

Figure 4.8. Electrode length comparison for the N-N system.

4.1.4. Effect of Electric Field Frequency on Critical Voltage

In Figure 4.9, the effect of the frequency of the applied electric field (f) is shown. The results suggest a positive correlation between f and V_c. That is, when the frequency of the applied electric field increases, it becomes more difficult to destabilize the interface. There is a qualitative consistency between these results and the numerical data provided by Roberts and Kumar[25]. The proposed model in the work suggests that increasing frequency should have a stabilizing effect on the interface and therefore result in higher critical voltages.

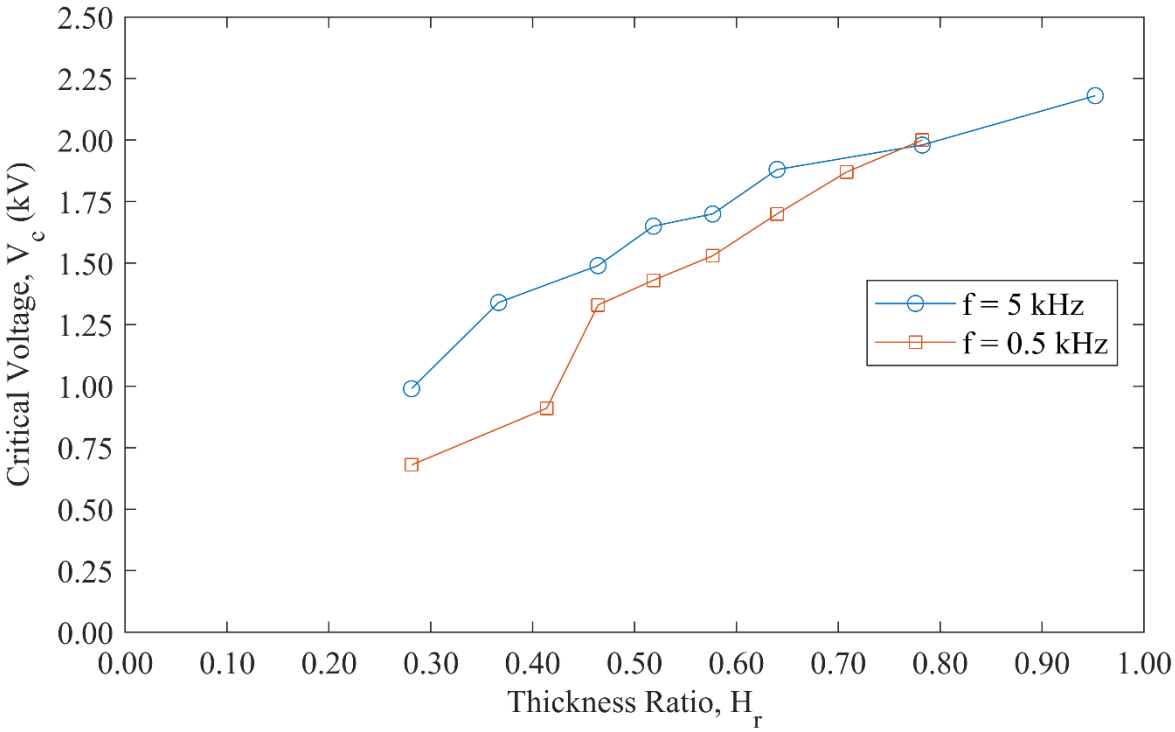

Figure 4.9. Electric field frequency comparison for the N-N system.

4.2. Electrohydrodynamic Instability for the Newtonian/non-Newtonian System

In this section, the thickness ratio H_r, and the critical voltage, V_c data of the Newtonian/non-Newtonian system are presented and discussed. For the N-nN system, this measurement is repeated three times and the averaged H_r is used as a controlled variable since the same Q_r inputs yielded quite consistent H_r outputs with the only exception of Q_r = 1.40, as opposed to the N-N system where the same Q_r inputs gave varying H_r results with relatively high standard deviations.

4.2.1. Effect of Volumetric Flow Rate Ratio on Thickness Ratio

In Figure 4.10, the average thickness ratio vs. flow rate ratio is plotted. As in the N-N system, there is a positive correlation between Q_r and H_r. The main difference, however, is that Q_r had to be held at relatively high values in order to obtain similar H_r readings to that of the N-N system. Namely, a Q_r input of 0.29 resulted in an average H_r value of 0.65 in the N-N system whereas the Q_r had to be held at 1.12 to obtain a similar H_r output of 0.64 in the N-nN system. Keeping in mind that Q_r and H_r are always the ratio of a property of Fluid 1

to a property Fluid 2, this suggests that the XG/AGl solution can push the silicone oil phase against the upper wall much better than ethylene glycol since glycerol has a higher viscosity (See Table 3.1). The measurement of H_r vs. Q_r was performed three times and the averaged values of H_r are shown in the plot (Figure 4.10).

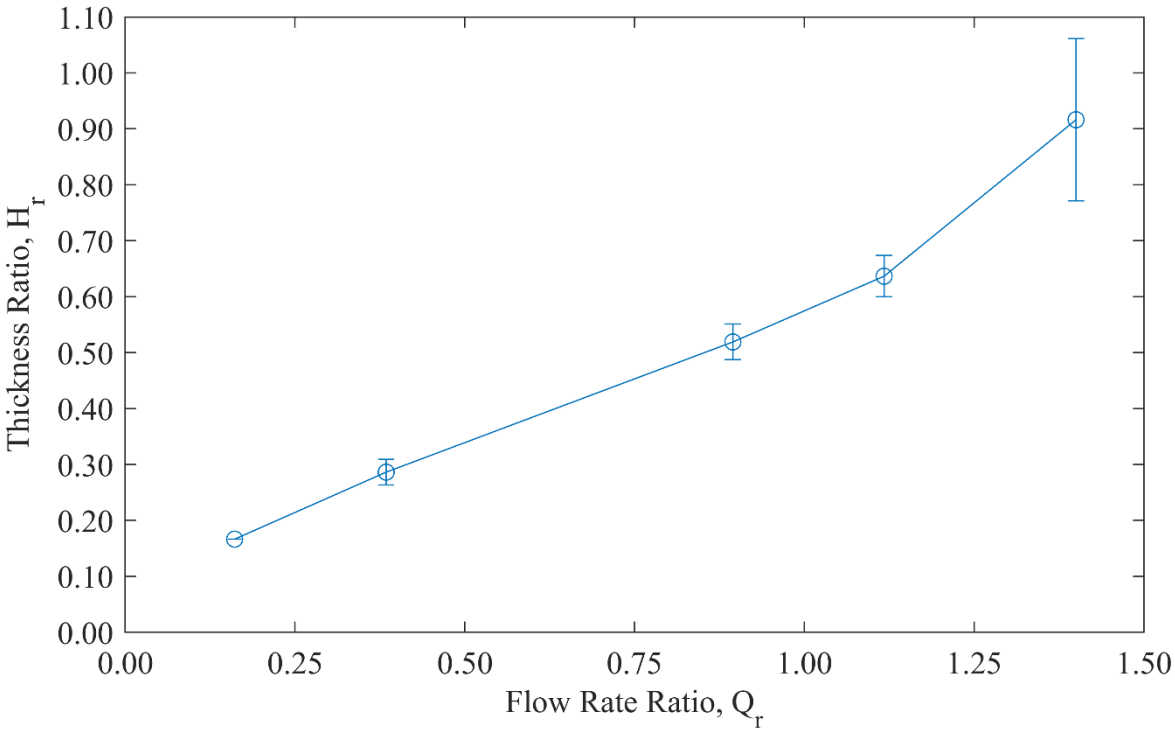

Figure 4.10. Average thickness ratio vs. flow rate ratio for N-nN systems.

4.2.2. Effect of Thickness Ratio on Critical Voltage

In Figure 4.11, the critical voltage is plotted against the averaged thickness ratios. When compared to the N-N system, the interface between a Newtonian and a non-Newtonian liquid is destabilized at higher voltages at similar H_r. e.g., V_c = 2.18 kV for H_r = 0.95 in the N-N system (Figure 4.5), whereas V_c = 2.63 kV for H_r = 0.92 in the N-nN system.

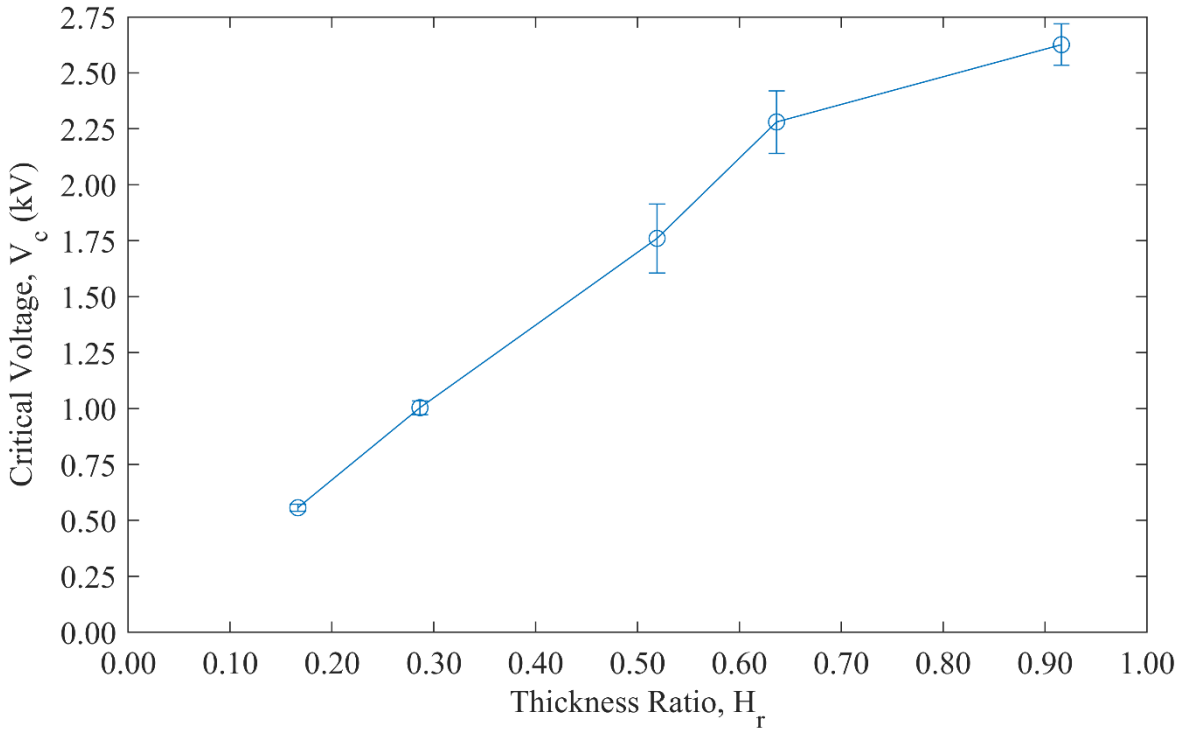

Figure 4.11. The effect of thickness ratio on critical voltage in the N-nN systems.

4.3. Droplet Formation in the Newtonian/non-Newtonian System

As mentioned earlier, for the N-nN systems once V_c is reached, the interface between the liquids hit the wall of the microchannel; but, does not generate droplets. When the applied voltage is sufficiently above V_c, the interface hits the wall at the entrance of the electrode (Figure 4.12a) creating a pocket of the dispersed phase. This pocket, then, starts moving along with the flow, growing in volume (Figure 4.12b). Finally, the thickness of the dispersed phase decreases at the back of the pocket (Figure 4.12c) and hits the upper wall at the electrode entrance a second time (Figure 4.12d), creating a droplet. This process is repeated periodically for every droplet formed.

Periodic formation of droplets was observed only at low values of H_r, namely, at 0.17, and 0.27, as for larger values of H_r (0.52, 0.64 and 0.92), the microchannels could not withstand high voltages necessary to generate droplets of constant size and period.

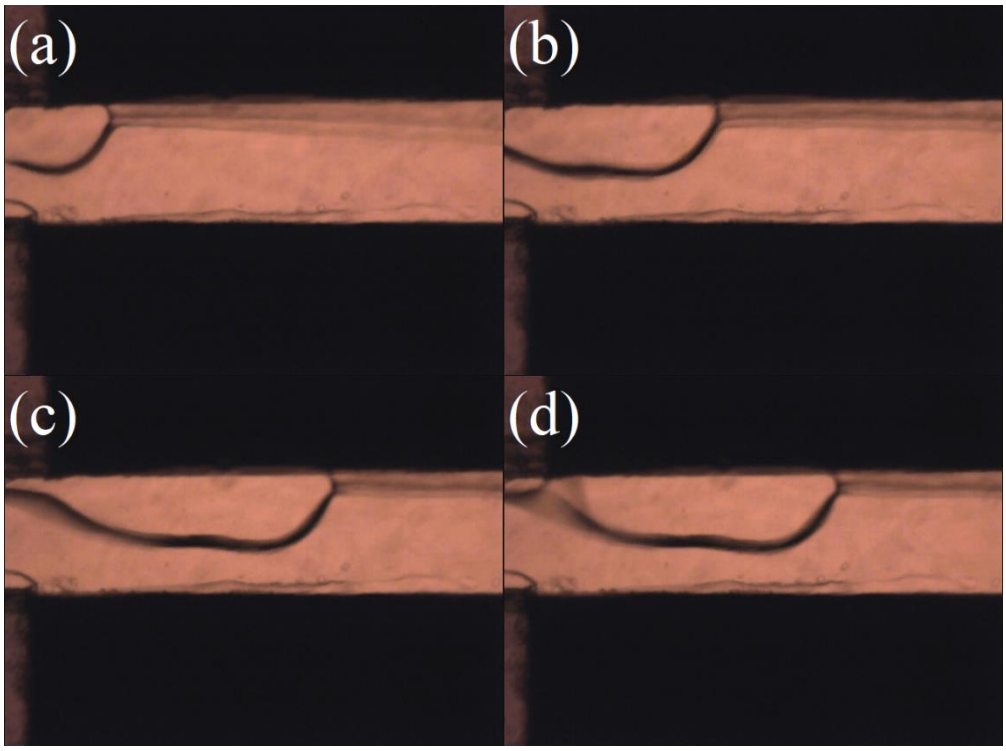

Figure 4.12. Formation of droplets in the N-nN system. (a) First flap against the upper wall, (b) growing, (c) thinning of the dispersed phase, (d) flapping against the wall a second time to form a droplet.

4.3.1. Droplet Formation, Size and Frequency

At the thickness ratio, H_r of 0.17, the critical voltage V_c is measured as 0.56 kV. However, the interface started generating droplets at and above 0.96 kV. The droplet sizes are measured at 0.96, 1.36, 1.76, 2.56 and 3.06 kV and the average droplet volumes ($V_{droplet}$) are measured as 0.499, 0.490, 0.479, 0.452 and 0.441 μL, respectively. For each value of the applied voltage (V), several droplets are sampled. Their calculated volumes are recorded along with the numbers of frames at which they are formed. The $V_{droplet}$ vs. Frame plot for H_r = 0.17 and the size comparison of the formed droplets can be seen in Figure 4.13 and 4.14, respectively. The vertical axis of the graph shows the volume of each droplet, and the horizontal distance between each data point shows how many frames passed between the generation of two consecutive droplets. The increasing values of the applied voltage have a minute diminishing effect on the frequency of droplet formation. However, the increasing voltages cause the droplet size to shrink significantly.

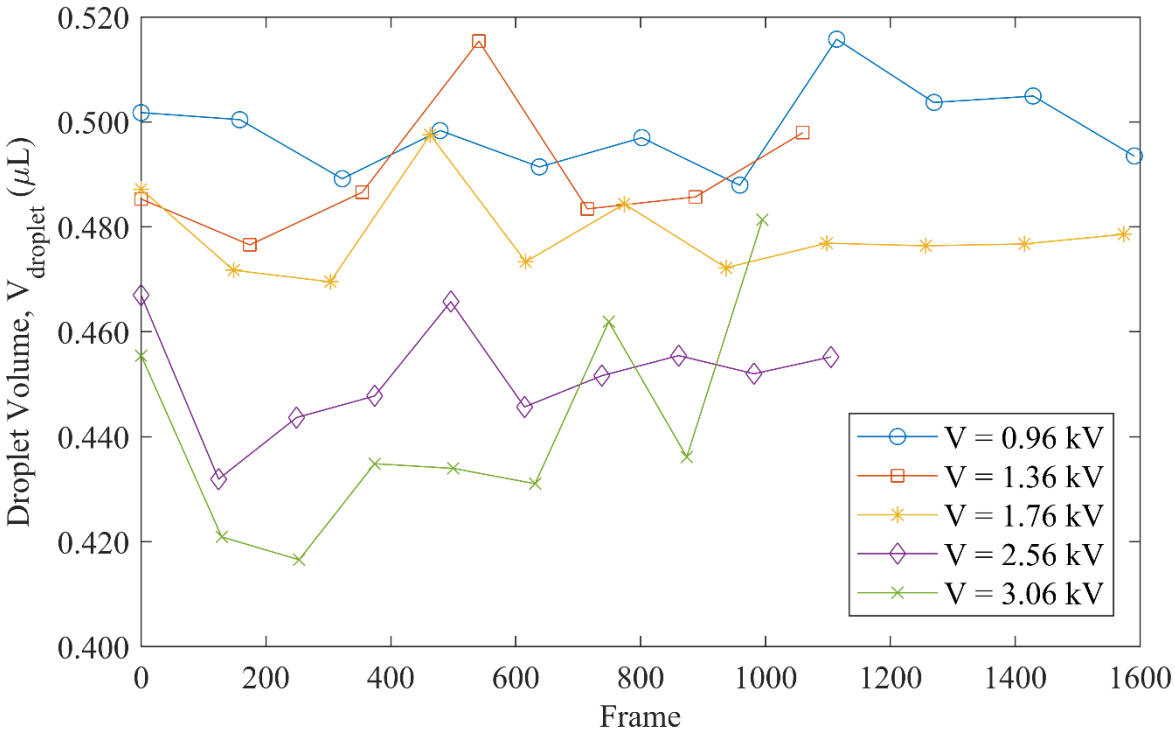

Figure 4.13. $V_{droplet}$ vs. Frame plot for H_r = 0.17.

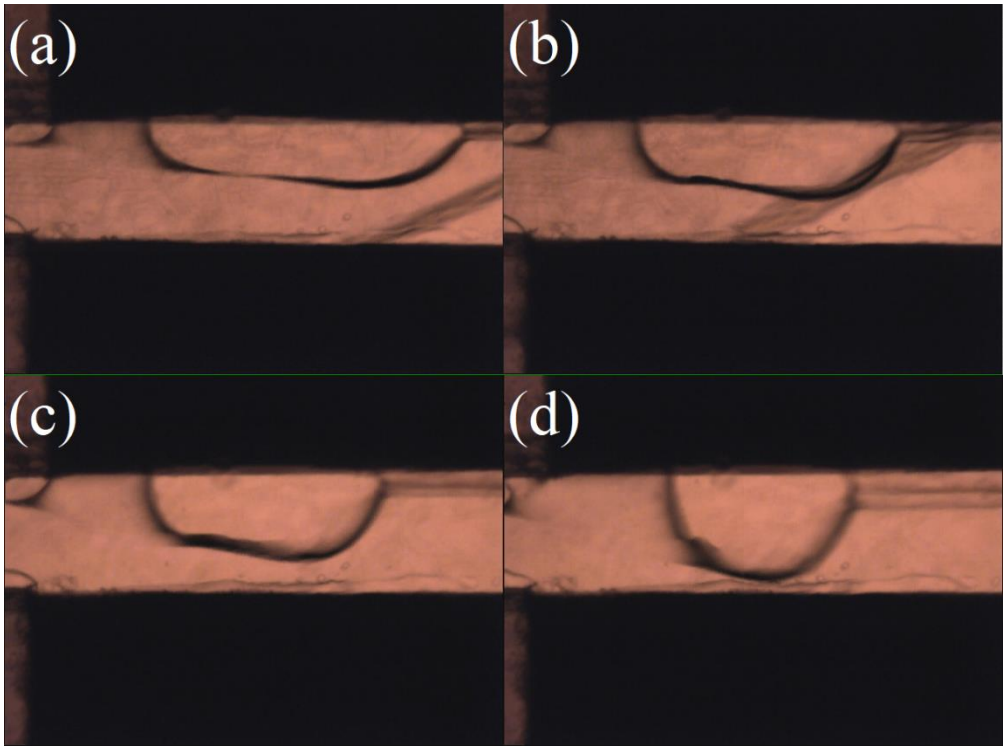

Figure 4.14. Size comparison of droplets at H_r = 0.17. (a) V = 0.96 kV, (b) V = 1.36 kV, (c) V = 1.76 kV, (d) V = 2.56 kV.

This procedure was repeated for H_r = 0.27 as well. This thickness ratio shows a similar pattern to the previous one except for V = 2.13 kV (Figures 4.15 and 4.16). At this voltage, the droplets formed were considerably bigger than and, consequently, stayed partially outside of the field of view of the microscope (12.50 mm).

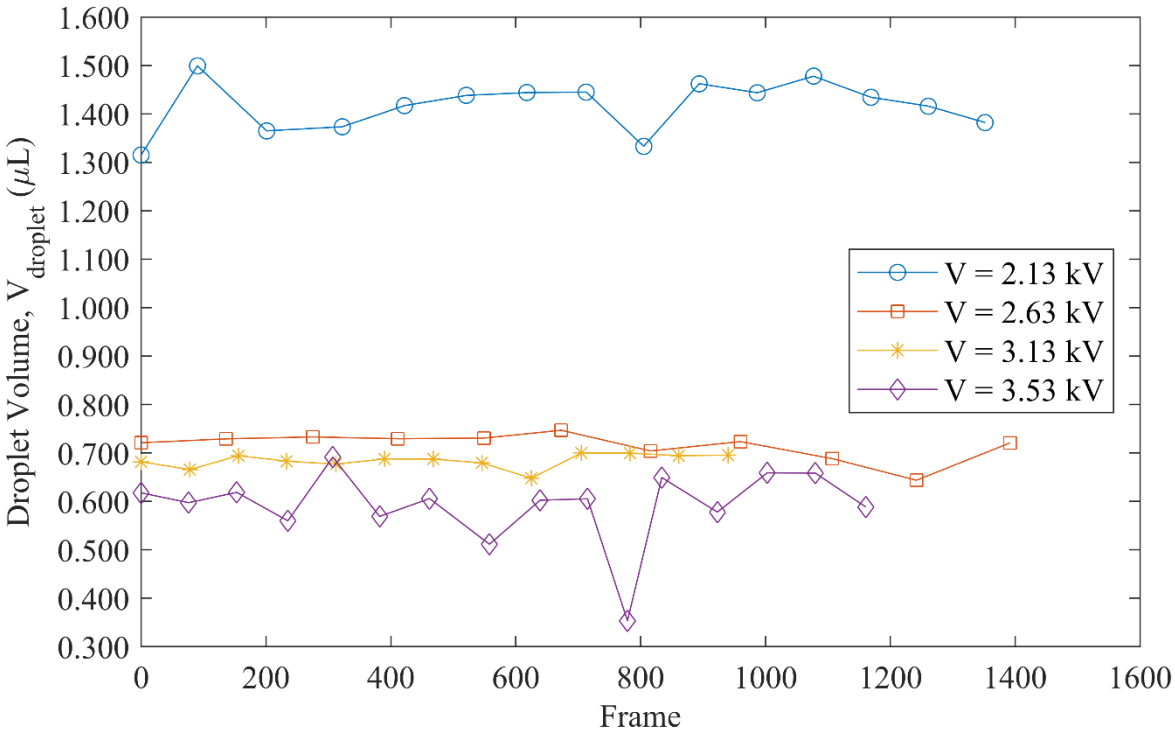

Figure 4.15. $V_{droplet}$ vs. Frame plot for H_r = 0.27.

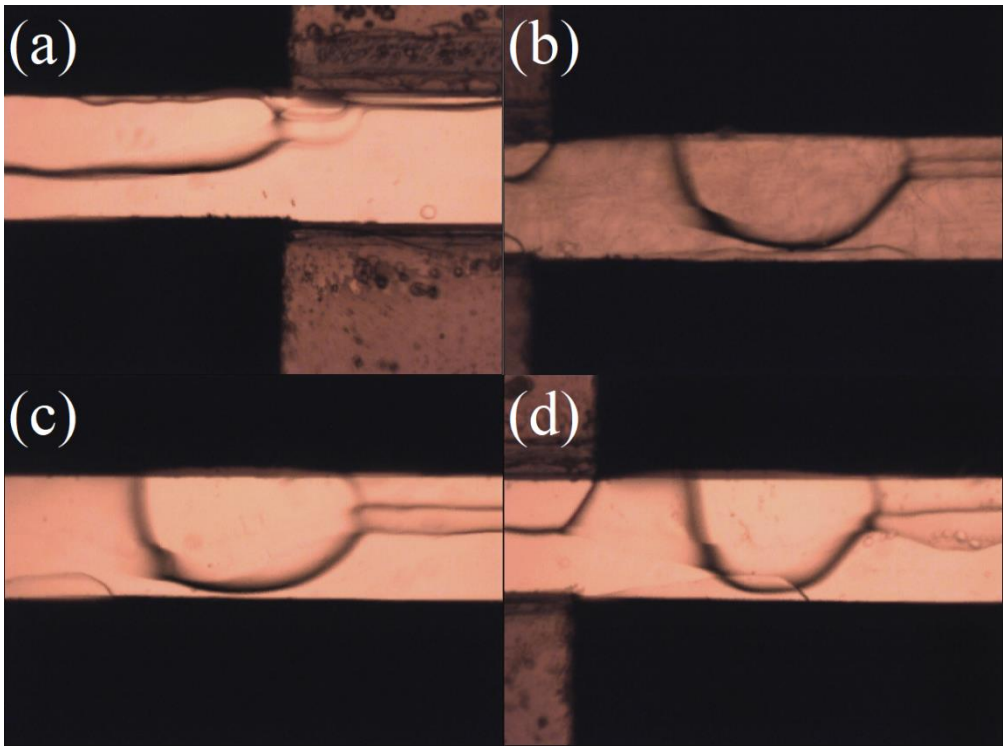

Figure 4.16. Size comparison of droplets at H_r = 0.17. (a) V = 2.13 kV, (b) V = 2.63 kV, (c) V = 3.13 kV, (d) V = 3.53 kV.

4.3.2. Effect of Applied Voltage on Droplet Size

In Figure 4.17 and 4.18, $V_{droplet}$ vs. V data are plotted for H_r = 0.17 and 0.27, respectively. In both configurations, the droplet size has a negative correlation with the applied voltage. This result is consistent with the experimental works of both Altundemir *et al.*[21] and Ozen *et al.*[17]. The main differences between the said works and these results are the choice of the continuous phase and the distribution of the droplet sizes which is more uniform (for two Newtonian liquids) as stated in the papers. However, it is worth mentioning that the continuous phase in both studies is a Newtonian liquid and the viscosity of the phase remains constant regardless of the varying shear rates in the flow. When the droplets of the dispersed phase are encapsulated by a shear-thinning non-Newtonian liquid[39], both the size and the frequency of the droplets could be affected by viscosity changes resulting from variations in the shear rate throughout the flow.

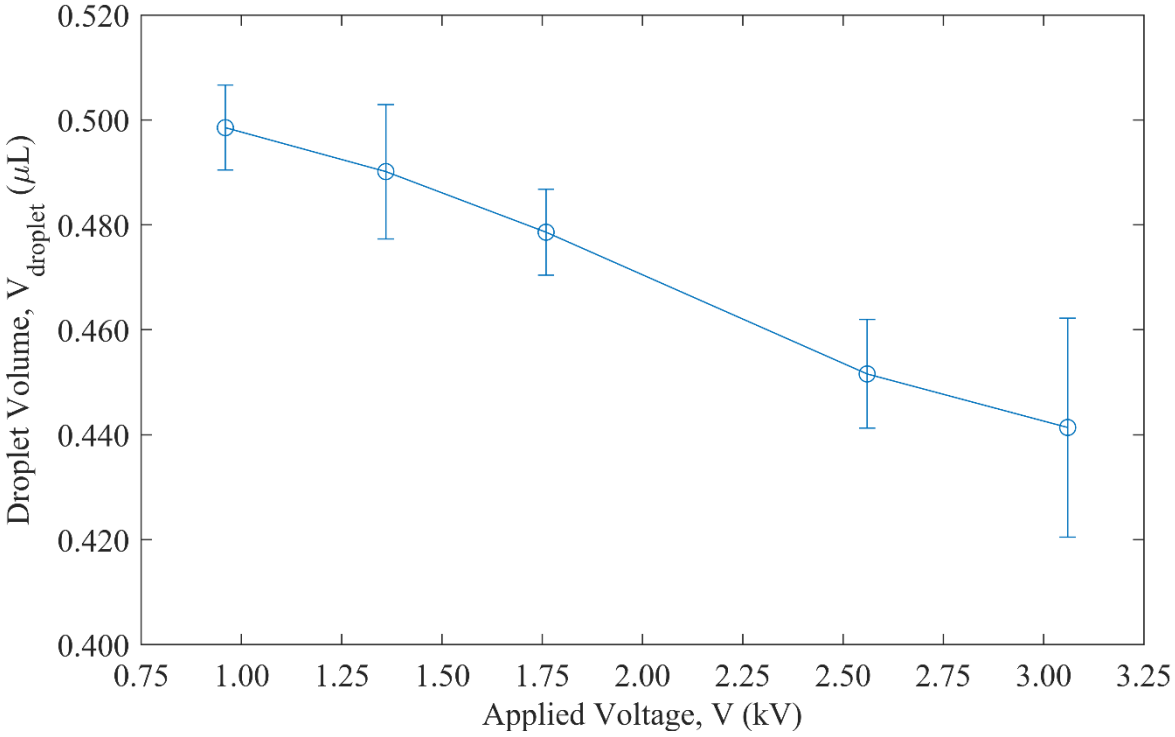

Figure 4.17. $V_{droplet}$ vs. V for H_r = 0.17.

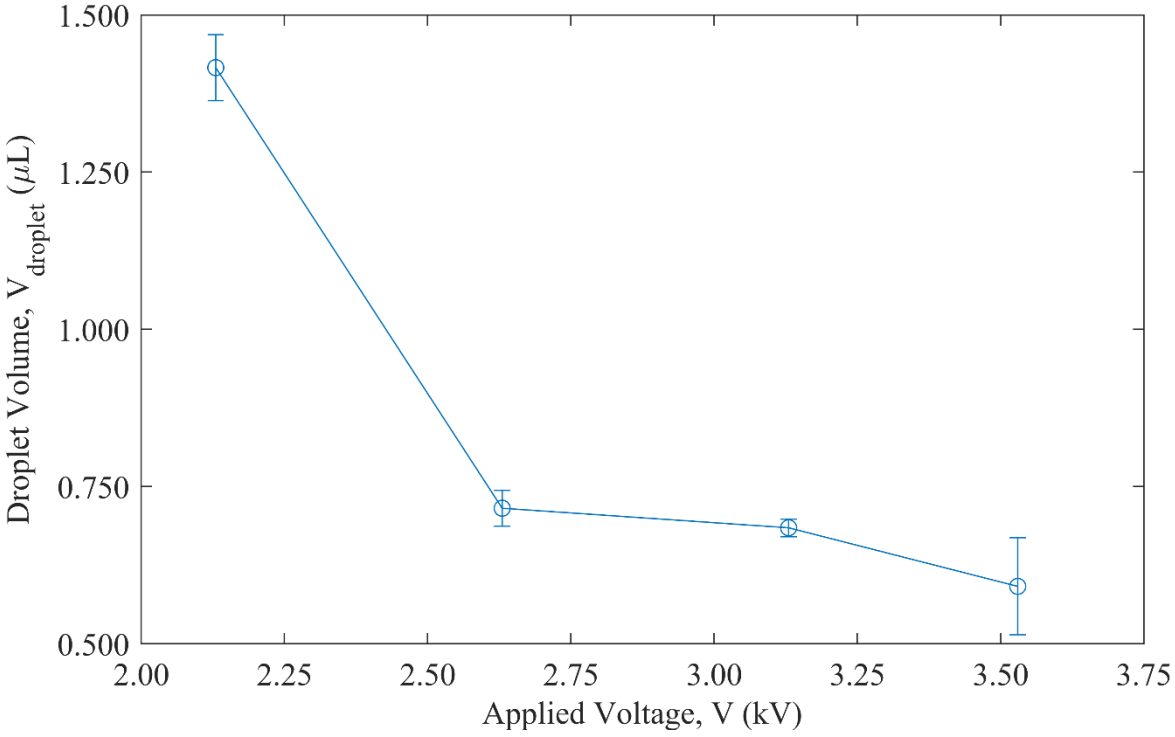

Figure 4.18. $V_{droplet}$ vs. V for H_r = 0.27.

5. CONCLUSIONS AND RECOMMENDATIONS

5.1. Conclusions

The electrohydrodynamic instability of the interface between two liquids flowing in a microchannel is studied experimentally in three parts. First, the distortion of the flat interface between two Newtonian (N-N system) liquids when it is subjected to an external AC electric field applied normal to the flat interface is investigated. Second, for the same experimental configuration, the N-N system is switched to a Newtonian and a non-Newtonian liquid (N-nN system). Finally, formation of droplets in the N-nN system with varying parameters is examined.

In the first part, the critical voltage at which the deflection of the interface between the liquids (N-N) is measured for three independent parameters, namely, the flow rate ratio, the frequency of the applied electric field and the electrode length. Here, the ratios are always defined as the property of the dispersed oil phase to that of continuous aqueous phase. The results indicate a positive and non-linear correlation between the volumetric flow rate ratio of the incoming phases and their thickness ratio. The thickness ratio has a stabilizing effect on the interface. That is, when the thickness ratio increases so does the voltage that is needed to destabilize the interface. Furthermore, the electrode length and the frequency of the applied electric field have a destabilizing and a stabilizing effect on the interface, respectively. Namely, the 20 mm electrode yielded critical voltages that are roughly 93 V less than that of the 10 mm electrode for similar values of the thickness ratio. Additionally, a 5 kHz AC electric field gave critical voltages which are 210 V, on average, more than that of a 0.5 kHz electric field.

In the second part, the critical voltage for the interface between a Newtonian and a non-Newtonian liquid is measured. The positive correlation between the thickness ratio and the flow rate ratio still holds. However, the flow rate ratios must be kept at relatively higher values in order to attain the same thickness ratios of the N-N system. This means, the xanthan gum/aqueous glycerol solution can push the dispersed phase silicone oil against the wall of the microchannel better than ethylene glycol can. This might be due to the higher viscosity

of the aqueous glycerol solution. In addition, the same flow rate ratios result in more consistent thickness ratios with lower standard deviations than that of the N-N system. There appears to be a clear distinction between the interface distortion mechanisms of the N-N and N-nN systems. In the N-N system, droplets are formed the moment the interface is destabilized and flaps against the wall. In the N-nN system, however, the interface hits against the wall of the microchannel and stops, taking another stable form. Only at voltages much higher than the critical voltage (400 V or more) does the N-nN system start generating droplets.

In the last part, droplet size is measured at varying thickness ratios and applied voltages. The system can produce droplets at low values of the thickness ratio (0.17, 0.27). Otherwise, the interface is too stable to allow droplet formation with critical voltages above 4 kV at which the integrity of the microchannel is not guaranteed. There is a negative correlation between the applied voltage and the droplet volume for both thickness ratios. In other words, higher values of the applied voltage resulted in smaller droplets. Furthermore, larger values of the thickness ratio result in bigger droplets. Namely, the H_r = 0.17 configuration generated droplets that are 0.441 to 0.499 μL in volume whereas the H_r = 0.27 configuration generated those that are 0.594 to 1.416 μL in volume.

5.2. Recommendations

In determining the critical voltage for the destabilization of the Newtonian/Newtonian interface three parameters are considered, namely, the thickness ratio, the electrode length and the frequency of the applied electric field. Although the experimental work provided good comparison between the outcomes of different values of the controlled parameters, the range of these parameters can be extended in order to observe the critical voltage vs. thickness ratio behavior of the interface at extremes, i.e., whether or not the critical voltage approaches a finite value as the thickness ratio goes to zero and/or infinity; i.e., as one liquid occupies the full channel. Additionally, the trend of the critical voltage can be understood when the electrode length is increased further. The work can be extended to determine the effect of the frequencies of the electric field on the stability of the interface. In addition, inclusion of the effect of other parameters such as the viscosity of the dispersed phase, the

channel depth, the total flow rate and the waveform should favor the applicability of the work.

The measured critical voltages to destabilize the Newtonian/non-Newtonian interface are relatively high for the microchannel to retain its integrity. To maintain lower critical voltages, a less viscous solvent can be chosen for the non-Newtonian phase. Furthermore, the effect of the xanthan gum concentration on the shear-thinning nature of the solution, the critical voltage and the average droplet size can be analyzed. The viscosity of the dispersed phase and its effects on the said parameters can be factored in.

In determining the ranges for the parameters in all three sets of measurements, the value of the voltage that can be applied to the microchannel without compromising its integrity was the major constraint. This issue can be rectified by using better constructed microchannels, relying more on welding, molding and unibody channel designs and less on adhesives which can be damaged via absorption of the incoming liquids and electrical currents allowing leakages, and can contaminate the liquids used in the experiments.

REFERENCES

1. G. M. Whitesides, “The origins and the future of microfluidics,” *Nature*, vol. 442, no. 7101, pp. 368–373, 2006.

2. G. S. Fiorini and D. T. Chiu, “Disposable microfluidic devices: fabrication, function, and application.,” *Biotechniques*, vol. 38, no. 3, pp. 429–46, Mar. 2005.

3. A. E. Kamholz, B. H. Weigl, B. A. Finlayson, and P. Yager, “Quantitative analysis of molecular interaction in a microfluidic channel: the T-sensor.,” *Anal. Chem.*, vol. 71, no. 23, pp. 5340–7, Dec. 1999.

4. Y. Jun Kang, J. Ryu, and S.-J. Lee, “Label-free viscosity measurement of complex fluids using reversal flow switching manipulation in a microfluidic channel,” *Biomicrofluidics*, vol. 7, no. 4, p. 044106, Jul. 2013.

5. E. B. Magnusson, S. Halldorsson, R. M. T. Fleming, and K. Leosson, “Real-time optical pH measurement in a standard microfluidic cell culture system.,” *Biomed. Opt. Express*, vol. 4, no. 9, pp. 1749–58, 2013.

6. D. Sparks *et al.*, “A microfluidic system for the measurement of chemical concentration and density,” in *TRANSDUCERS 2003 - 12th International Conference on Solid-State Sensors, Actuators and Microsystems, Digest of Technical Papers*, 2003, vol. 1, pp. 300–303.

7. P. S. Bulutoglu, S. Koc, and A. K. Avci, “Simulation of exhaust gas reforming of natural gas in a microchannel reactor,” *Int. J. Hydrogen Energy*, vol. 41, no. 19, pp. 8184–8192, May 2016.

8. T. Y. Seo *et al.*, “Immobilized cell microchannel bioreactor for evaluating fermentation characteristics of mixed substrate consumption and product formation,” 2012.

9. A. Y. Hsiao *et al.*, “Microfluidic system for formation of PC-3 prostate cancer co-culture spheroids,” *Biomaterials*, vol. 30, no. 16, pp. 3020–3027, Jun. 2009.

10. E. T. Lagally, P. C. Simpson, and R. A. Mathies, “Monolithic integrated microfluidic DNA amplification and capillary electrophoresis analysis system,” *Sensors Actuators B Chem.*, vol. 63, no. 3, pp. 138–146, May 2000.

11. A. Xiang *et al.*, “An aptamer-based immunoassay in microchannels of a portable analyzer for detection of microcystin-leucine-arginine,” *Talanta*, vol. 130, pp. 363–369, Dec. 2014.

12. T. Nisisako, T. Torii, and T. Higuchi, “Droplet formation in a microchannel network,” in *Lab on a Chip*, 2002, vol. 2, no. 1, pp. 24–26.

13. J. Atencia and D. J. Beebe, “Controlled microfluidic interfaces,” *Nature*, vol. 437, no. 7059, pp. 648–655, Sep. 2005.

14. N. Schwesinger, T. Frank, and H. Wurmus, “A modular microfluid system with an integrated micromixer,” *J. Micromechanics Microengineering*, vol. 6, no. 1, pp. 99–102, Mar. 1996.

15. D. R. Link, S. L. Anna, D. A. Weitz, and H. A. Stone, “Geometrically Mediated Breakup of Drops in Microfluidic Devices,” *Phys. Rev. Lett.*, vol. 92, no. 5, p. 4, 2004.

16. S. L. Anna, N. Bontoux, and H. A. Stone, “Formation of dispersions using ‘flow focusing’ in microchannels,” *Appl. Phys. Lett.*, vol. 82, no. 3, pp. 364–366, 2003.

17. O. Ozen, N. Aubry, D. T. Papageorgiou, and P. G. Petropoulos, “Monodisperse drop formation in square microchannels,” *Phys. Rev. Lett.*, vol. 96, no. 14, pp. 1–4, 2006.

18. X. Casadevall Solvas and A. deMello, “Droplet microfluidics: recent developments and future applications,” *Chem. Commun*, vol. 47, pp. 1936–1942, 2011.

19. H. A. Stone, A. D. Stroock, and A. Ajdari, “Engineering Flows in Small Devices,” *Annu. Rev. Fluid Mech.*, vol. 36, no. 1, pp. 381–411, 2004.

20. X. Casadevall I Solvas and A. Demello, “Droplet microfluidics: Recent developments and future applications,” *Chem. Commun.*, vol. 47, no. 7, pp. 1936–1942, 2011.

21. S. Altundemir, P. Eribol, and K. Uguz, “Droplet formation and its mechanism in a microchannel in the presence of an electric field,” *Fluid Dyn. Res.*, 2018.

22. D. A. Saville, “Electrohydrodynamics:The Taylor-Melcher Leaky Dielectric Model,” *Annu. Rev. Fluid Mech.*, vol. 29, no. 1, pp. 27–64, 1997.

23. K. Abdella and H. Rasmussen, “Electrohydrodynamic instability of two superposed fluids in normal electric fields,” *J. Comput. Appl. Math.*, vol. 78, no. 1, pp. 33–61, 1997.

24. O. Ozen, N. Aubry, D. T. Papageorgiou, and P. G. Petropoulos, “Electrohydrodynamic linear stability of two immiscible fluids in channel flow,” *Electrochim. Acta*, vol. 51, no. 25, pp. 5316–5323, 2006.

25. S. A. Roberts and S. Kumar, “AC electrohydrodynamic instabilities in thin liquid films,” *J. Fluid Mech.*, vol. 631, no. 2010, pp. 255–279, 2009.

26. A. K. Uguz, O. Ozen, and N. Aubry, “Electric field effect on a two-fluid interface instability in channel flow for fast electric times,” *Phys. Fluids*, vol. 20, no. 3, 2008.

27. A. Sharma, J. Chaudhuri, V. Kumar, S. Timung, T. K. Mandal, and D. Bandyopadhyay, “Digitization of two-phase flow patterns in a microchannel induced by an external AC field,” *RSC Adv.*, vol. 5, no. 37, pp. 29545–29551, 2015.

28. P. Eribol and A. K. Uguz, “Experimental investigation of electrohydrodynamic instabilities in micro channels,” *Eur. Phys. J. Spec. Top.*, vol. 224, no. 2, pp. 425–434, 2015.

29. L. Haiwang, W. Teck Neng, and N. Nam-Trung, “Electrohydrodynamic and Shear-Stress Interfacial Instability of Two Streaming Viscous Liquid Inside a Microchannel for Tangential Electric Fields,” *Micro Nanosyst.*, vol. 4, no. 1, pp. 14–24, 2012.

30. H. Li, T. N. Wong, and N. T. Nguyen, “Instability of pressure driven viscous fluid streams in a microchannel under a normal electric field,” *Int. J. Heat Mass Transf.*, vol. 55, no. 23–24, pp. 6994–7004, 2012.

31. P. Gambhire and R. M. Thaokar, “Electrohydrodynamic instabilities at interfaces subjected to alternating electric field,” *Phys. Fluids*, vol. 22, no. 6, pp. 1–16, 2010.

32. S. A. Roberts and S. Kumar, “Electrohydrodynamic instabilities in thin liquid trilayer films Electrohydrodynamic instabilities in thin liquid trilayer films,” vol. 122102, no. 2010, 2014.

33. S. Y. Teh, R. Lin, L. H. Hung, and A. P. Lee, “Droplet microfluidics,” *Lab on a Chip*, vol. 8, no. 2. The Royal Society of Chemistry, pp. 198–220, Jan-2008.

34. H. Gu, M. H. G. Duits, and F. Mugele, “Droplets formation and merging in two-phase flow microfluidics,” *Int. J. Mol. Sci.*, vol. 12, no. 4, pp. 2572–2597, 2011.

35. J. K. Nunes, S. S. H. Tsai, J. Wan, and H. A. Stone, “Dripping and jetting in microfluidic multiphase flows applied to particle and fibre synthesis,” *J. Phys. D. Appl. Phys.*, vol. 46, no. 11, 2013.

36. S. Okushima, T. Nisisako, T. Torii, and T. Higuchi, “Controlled production of monodisperse double emulsions by two-step droplet breakup in microfluidic devices,” *Langmuir*, vol. 20, no. 23, pp. 9905–9908, 2004.

37. N. T. Nguyen *et al.*, “Thermally mediated droplet formation in microchannels,” *Appl. Phys. Lett.*, vol. 91, no. 8, pp. 89–92, 2007.

38. S. H. Tan, N. T. Nguyen, L. Yobas, and T. G. Kang, “Formation and manipulation of ferrofluid droplets at a microfluidic T-junction,” *J. Micromechanics Microengineering*, vol. 20, no. 4, 2010.

39. M. Khagram, R. K. Gupta, and T. Sridhar, “Extensional Flow of Xanthan Gum Solutions,” *J. Rheol. (N. Y. N. Y).*, vol. 29, no. 2, pp. 191–207, 2002.

APPENDIX A: Q_R, H_R AND V_C DATA OF THE NEWTONIAN / NEWTONIAN SYSTEMS

Table A.1. Data of the Configuration with L_e = 10 mm and f = 5 kHz.

Run #	Q_1 (µL/min)	Q_2 (µL/min)	Q_r	H_1	H_2	H_r	V_c (kV)
1	50	130	0.38	2.0	2.1	0.95	2.18
2	45	135	0.33	1.8	2.3	0.78	1.98
3	40	140	0.29	1.6	2.5	0.64	1.88
4	35	145	0.24	1.5	2.6	0.58	1.70
5	30	150	0.20	1.4	2.7	0.52	1.65
6	25	155	0.16	1.3	2.8	0.46	1.49
7	20	160	0.13	1.1	3.0	0.37	1.34
8	15	165	0.09	0.9	3.2	0.28	0.99

Table A.2 Data of the Configuration with L_e = 20 mm and f = 5 kHz.

Run #	Q_1 (µL/min)	Q_2 (µL/min)	Q_r	H_1	H_2	H_r	V_c (kV)
1	50	130	0.38	1.6	2.2	0.73	1.87
2	45	135	0.33	1.5	2.3	0.65	1.78
3	40	140	0.29	1.4	2.4	0.58	1.69
4	35	145	0.24	1.3	2.5	0.52	1.59
5	30	150	0.20	1.2	2.6	0.46	1.29

Table A.3 Data of the Configuration with L_e = 10 mm and f = 0.5 kHz.

Run #	Q_1 (µL/min)	Q_2 (µL/min)	Q_r	H_1	H_2	H_r	V_c (kV)
1	50	130	0.38	1.8	2.3	0.78	2.00
2	45	135	0.33	1.7	2.4	0.71	1.87
3	40	140	0.29	1.6	2.5	0.64	1.70
4	35	145	0.24	1.5	2.6	0.58	1.53
5	30	150	0.20	1.4	2.7	0.52	1.43
6	25	155	0.16	1.3	2.8	0.46	1.33
7	20	160	0.13	1.2	2.9	0.41	0.91
8	15	165	0.09	0.9	3.2	0.28	0.68

APPENDIX B: Q_R, H_R AND V_C DATA OF THE NEWTONIAN / NON-NEWTONIAN SYSTEMS

Table B.1. Data of the First Set at Default L_e and f.

Run #	Q_1 (µL/min)	Q_2 (µL/min)	Q_r	H_1	H_2	H_r	V_c (kV)
1	105	75	1.40	2.1	2.1	1.00	2.60
2	95	85	1.12	1.6	2.6	0.62	2.18
3	85	95	0.89	1.4	2.8	0.50	1.72
4	50	130	0.38	1.0	3.2	0.31	1.01
5	25	155	0.16	0.6	3.6	0.17	0.56

Table B.2. Data of the Second Set at Default L_e and f.

Run #	Q_1 (µL/min)	Q_2 (µL/min)	Q_r	H_1	H_2	H_r	V_c (kV)
1	105	75	1.40	2.1	2.1	1.00	2.73
2	95	85	1.12	1.6	2.6	0.62	2.22
3	85	95	0.89	1.4	2.8	0.50	1.93
4	50	130	0.38	0.9	3.3	0.27	0.97
5	25	155	0.16	0.6	3.6	0.17	0.57

Table B.3. Data of the Third Set at Default L_e and f.

Run #	Q_1 (µL/min)	Q_2 (µL/min)	Q_r	H_1	H_2	H_r	V_c (kV)
1	105	75	1.40	1.8	2.4	0.75	2.55
2	95	85	1.12	1.7	2.5	0.68	2.44
3	85	95	0.89	1.5	2.7	0.56	1.63
4	50	130	0.38	0.9	3.3	0.27	1.03
5	25	155	0.16	0.6	3.6	0.17	0.54

APPENDIX C: DROPLET SIZE DATA OF THE NEWTONIAN / NON-NEWTONIAN SYSTEM

Table C.1. Data of the Configuration with H_r = 0.17 and V = 0.96 kV.

Droplet #	Entrance Frame #	$V_{droplet}$ (μL)
1	0	0.502
2	158	0.500
3	322	0.489
4	479	0.498
5	638	0.491
6	802	0.497
7	959	0.488
8	1114	0.516
9	1270	0.504
10	1429	0.505
11	1591	0.493
Average		0.499
Standard Deviation		0.008

Table C.2. Data of the Configuration with H_r = 0.17 and V = 1.36 kV.

Droplet #	Entrance Frame #	$V_{droplet}$ (μL)
1	0	0.485
2	174	0.477
3	354	0.487
4	541	0.515
5	715	0.483
6	888	0.486
7	1060	0.498
Average		0.490
Standard Deviation		0.013

Table C.3. Data of the Configuration with H_r = 0.17 and V = 1.76 kV.

Droplet #	Entrance Frame #	$V_{droplet}$ (μL)
1	0	0.487
2	148	0.472
3	303	0.470
4	463	0.498
5	616	0.473
6	774	0.484
7	937	0.472
8	1098	0.477
9	1257	0.476
10	1415	0.477
11	1574	0.479
Average		0.479
Standard Deviation		0.008

Table C.4. Data of the Configuration with H_r = 0.17 and V = 2.56 kV.

Droplet #	Entrance Frame #	$V_{droplet}$ (μL)
1	0	0.467
2	124	0.432
3	249	0.444
4	374	0.448
5	496	0.466
6	614	0.446
7	738	0.452
8	861	0.455
9	982	0.452
10	1105	0.455
Average		0.452
Standard Deviation		0.010

Table C.5. Data of the Configuration with H_r = 0.17 and V = 3.06 kV.

Droplet #	Entrance Frame #	$V_{droplet}$ (μL)
1	0	0.455
2	129	0.421
3	253	0.417
4	374	0.435
5	500	0.434
6	631	0.431
7	749	0.462
8	874	0.436
9	995	0.481
Average		0.441
Standard Deviation		0.021

Table C.6. Data of the Configuration with H_r = 0.27 and V = 2.13 kV.

Droplet #	Entrance Frame #	$V_{droplet}$ (μL)
1	0	1.315
2	90	1.499
3	201	1.365
4	322	1.373
5	422	1.417
6	521	1.438
7	618	1.444
8	713	1.445
9	805	1.333
10	894	1.462
11	987	1.444
12	1077	1.478
13	1169	1.434
14	1261	1.416
15	1352	1.382
Average		1.416
Standard Deviation		0.053

Table C.7. Data of the Configuration with H_r = 0.27 and V = 2.63 kV.

Droplet #	Entrance Frame #	$V_{droplet}$ (μL)
1	0	0.721
2	136	0.729
3	275	0.733
4	411	0.729
5	549	0.731
6	673	0.747
7	816	0.704
8	960	0.723
9	1107	0.688
10	1242	0.644
11	1392	0.721
Average		0.715
Standard Deviation		0.028

Table C.8. Data of the Configuration with H_r = 0.27 and V = 3.13 kV.

Droplet #	Entrance Frame #	$V_{droplet}$ (μL)
1	-	0.687
2	0	0.682
3	78	0.666
4	156	0.694
5	233	0.683
6	312	0.677
7	390	0.687
8	468	0.687
9	546	0.679
10	625	0.648
11	705	0.700
12	783	0.700
13	861	0.694
14	940	0.695
Average		0.684
Standard Deviation		0.014

Table C.9. Data of the Configuration with H_r = 0.27 and V = 3.53 kV.

Droplet #	Entrance Frame #	$V_{droplet}$ (μL)
1	0	0.618
2	76	0.597
3	153	0.619
4	235	0.560
5	307	0.691
6	382	0.569
7	462	0.606
8	558	0.512
9	639	0.602
10	715	0.605
11	779	0.353
12	834	0.649
13	923	0.578
14	1003	0.659
15	1080	0.658
16	1161	0.588
Average		0.592
Standard Deviation		0.077